Graphitic carbon nitride meets molecular oxygen: New sustainable photocatalytic ways for the oxidation of organic molecules

Gaia Grando [a,‡], Giuseppe Sportelli [a,b,‡], Giacomo Filippini [a,*], Michele Melchionna [a,c,*], Paolo Fornasiero [a,c,*]

[a] Department of Chemical and Pharmaceutical Sciences, University of Trieste, via Licio Giorgieri 1, Trieste 34127, Italy
[b] Department of Science, Technology and Society, University School for Advanced Studies IUSS Pavia, Piazza della Vittoria 15, Pavia 27100, Italy
[c] Center for Energy, Environment and Transport "Giacomo Ciamician" and ICCOM-CNR Trieste Research Unit, University of Trieste, via Licio Giorgieri 1, Trieste 34127, Italy

ABSTRACT

In recent years, organic chemists have taken a resolute step toward green photocatalytic synthesis. In this regard, the oxidation of organic compounds with molecular oxygen is one of the most important classes of transformations, as it increases molecular complexity while avoiding the use of toxic and harmful oxidants. To this aim, the development of new and efficient photocatalysts capable of driving valuable oxidative reactions in a sustainable manner is highly desirable. These novel photocatalytic systems need to be metal-free, easy-to-prepare, and potentially recyclable. Carbon nitride (CN) fulfills all these requirements because of its outstanding physicochemical properties, thus emerging as a promising heterogeneous photocatalytic platform. The growing popularity of this material is also substantiated by its fast and facile preparation from readily available and inexpensive molecular precursors. This Review aims at highlighting the recent advances in synthesis of carbon nitride-based materials and their applications in organic photocatalysis for the oxidation of organic molecules in presence of molecular oxygen. Lastly, forward-looking opportunities within this intriguing research field are mentioned.

1. Introduction

Oxidation reactions play a crucial role in the synthesis of different organic molecules of great industrial relevance. For example, many industrially relevant monomers in polymer chemistry (such as terephthalic acid, ε-caprolactam, among others) can be easily produced through oxidative processes (Fig. 1) [1]. In parallel, selective and atom-economical large scale oxidative transformations of organic compounds are of enormous interest for the development of new active ingredients (see Fig. 1) in the pharmaceutical companies [2–5].

However, a number of these processes are still based on old-fashioned chemical approaches, which generally rely on the use of precious and potentially toxic metal-based species and/or on the exploitation of stoichiometric amounts of oxidants [1,6,7]. Nonetheless, the rising social and political awareness about environmental issues is steering industries to move towards greener and more sustainable strategies, thus attempting to adhere to Green Chemistry principles [1,

7]. Set in 1998 by Anastas and Warner, 'Green Chemistry' defines a compendium of twelve rules that serve as a source of inspiration for the design of novel reactions with little environmental impact [8,9]. In line with these principles, researchers are challenged to find new synthetic routes that prevent or reduce the production of wastes and toxic by-products [8,9]. In this context, catalysis has a fundamental role to solve arduous tasks in synthetic chemistry and is thus involved in the global economy in many industrial fields [9]. Semiconductors have a dominant role as photocatalysts for energy-related chemical processes, and in recent years their use has been extended to organic reactions, too. The photogenerated charge carriers (separated electrons and holes formed upon illumination with suitable wavelengths photons) in the semiconductors often interact with organic substrates by means of single-electron transfer (SET) steps that leads to reaction pathways of utility for target final compounds (Fig. 2) [10,11].
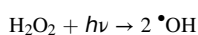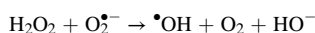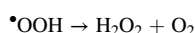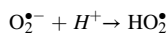
The direct oxidation of organic compounds with the photo-induced holes may take place only if molecules' redox potential fall above (on

the energy scale) the valence band edge [12]. An alternative path involves the photochemical generation of reactive oxygen species (ROS) from suitable precursors (*e.g.*, molecular oxygen), within the frame of the so-called 'Advanced Oxidation Processes' (AOPs). Despite the $^\bullet$OH radicals generated by water oxidation ($E^0(^\bullet OH/OH^-) = +2.72$ V *vs* normal hydrogen electrode, NHE) are too reactive and may end up to over oxidation pathways, the direct photoreduction of O_2 gives superoxide radicals ($O_2^{\bullet-}$, $E^0(O_2/O_2^{\bullet-}) = -0.33$ V at pH$= 7$ vs NHE) which are milder oxidants and can therefore react with appropriate organic functionalities leading to selective organic reactions [12,13]. Additionally, superoxide radicals can prompt the formation of secondary ROS, such as hydroperoxyl radicals ($^\bullet$OOH) and hydrogen peroxide (through a multiple electron-reduction mechanism) that can also contribute to the oxidation process [12,13].

$$O_2^{\bullet-} + H^+ \rightarrow HO_2^\bullet$$

$$^\bullet OOH \rightarrow H_2O_2 + O_2$$

$$H_2O_2 + O_2^{\bullet-} \rightarrow {}^\bullet OH + O_2 + HO^-$$

$$H_2O_2 + h\nu \rightarrow 2\,^\bullet OH$$

Alternatively, $O_2^{\bullet-}$ can undergo oxidation *via* the photogenerated holes, yielding also singlet oxygen ($^1O_2$) which may serve as mild oxidant, too [12]. Especially for polymeric semiconductors, it has been demonstrated that singlet oxygen can be afforded even through direct photosensitization. If an organic dye (or the semiconductor itself) can access a triplet state *via* intersystem crossing, the slowly released energy from the decay can be absorbed by O_2, promoting the formation of $^1O_2$ [14,15]. Since oxygen is widely abundant in the atmosphere, its usage for oxidation reactions should be encouraged in spite of other more polluting oxidants [8,16]. Thus, this review aims at critically highlight the importance of polymeric carbon nitride (PCN) and its derivatives as heterogeneous metal-free semiconducting platforms to perform photocatalytic oxidation of organic molecules.

2. Carbon nitride: a versatile photocatalytic platform

In the realm of semiconductors, PCN and its derivatives are appealing materials extensively studied for a wide range of applications, including heterogenous photocatalysis (see Fig. 3) [17]. Beyond the first synthetic report from Liebig and the earliest hypothesis about its
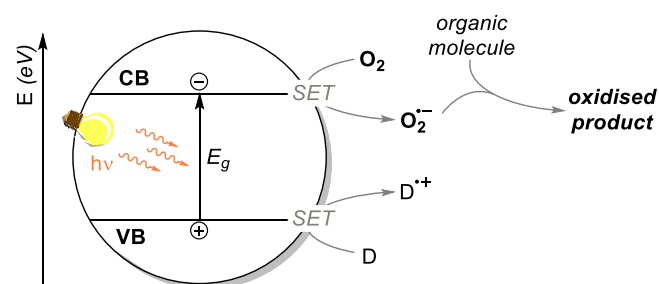

Fig. 2. Schematic representation of a generic semiconductor's band gap (aligned by increasing energy), with a focus on the activation of molecular oxygen towards oxidations. Single-electron transfer events are also hinted by means of arrows, so that we can differ between the electron-donor species (**D**, oxidized to the radical cation **D$^{\bullet+}$**) and the O$_2$, which is the electron-acceptor (**O$_2$**, reduced to its radical anion **O$_2^{\bullet-}$**). Subsequently, superoxide radicals can react with an organic compound, oxidizing it. VB$=$ valence band, CB$=$ conduction band, $E_g=$ band gap, SET$=$ single-electron transfer.

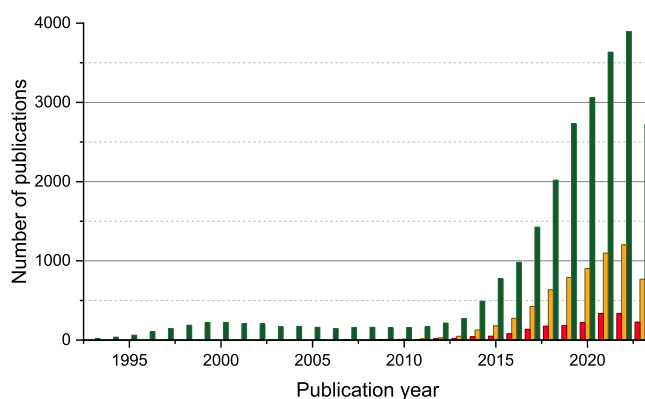**Fig. 3.** Number of publications per year (starting from 1993) using "carbon nitride" (green bars), "carbon nitride AND photocatalysis" (yellow bars) or "carbon nitride AND photocatalysis AND oxidation" (red bars) as search keywords on Web of Science™ (last updated: 04/11/2023).
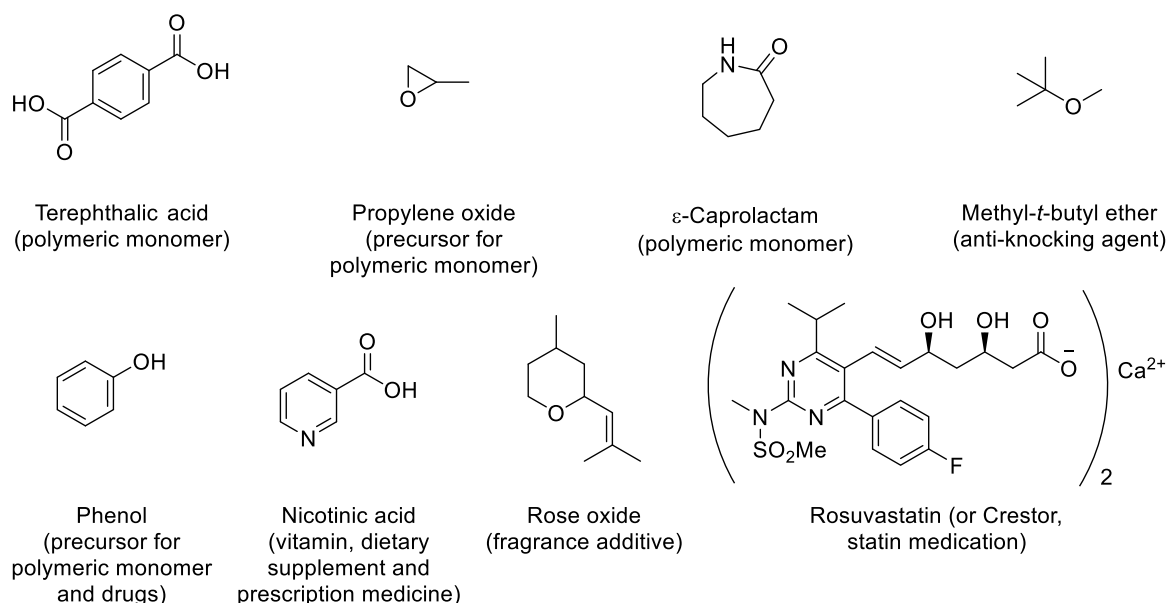

Fig. 1. Selected examples of industrially relevant organic molecules that require at least one oxidation step for their synthesis.

structure, [18–21] the use of PCN as a platform for driving light-induced chemical processes has boomed after that Antonietti, Domen and co-workers were able to perform the H₂ evolution reaction from water under visible light illumination in 2009 [22].

Since then, this pioneering work has paved the way for further photocatalytic applications which span from energy-related processes, such as H₂ production and CO₂ reduction, to organic synthesis for the sustainable production of valuable organic molecules [23–30]. The research in this field has been continuously increasing over the last decade, as shown in Fig. 3. From a structural point of view, PCN is proposed to be mainly constituted by a framework of N-bridged poly (tri-s-triazine) arranged into stacked and cross-linked graphite-like π-conjugated planar layers (although other repeating units have been proposed) [25,26]. Such morphology (and the related features) can be tuned by carrying out structural and chemical modifications (as we will discuss in the following sections), but what makes carbon nitrides really appealing for future applications is the ease of preparation as well as the large abundance of the constituting elements.

2.1. Preparation and thermal treatments

Carbon nitride can be easily obtained through simple and robust bottom-up synthetic protocols. These approaches generally are based on the poly-condensation (with loss of ammonia) at high temperatures of simple and commercially available nitrogen-rich molecules, such as cyanamide, dicyandiamide, urea and melamine (see, respectively, *i, ii, iii* and *iv* in Fig. 4) [25,26,31]. Nonetheless, several other precursors have been also explored in the material synthesis to bring specific moieties into the polymeric structure or to tune its final properties [25,26,31]. For instance, Savateev *et al.* observed that carbon nitride can be obtained also by means of a 'topotactic' transition of another C,N,H-containing polymer, such as poly(3-amino-1,2,4-triazole) [32]. As presented in Fig. 4, mechanistic investigations pointed out that polymerization proceeds stepwise: first, with the formation of melamine, when it is not the initial precursor, followed by the formation of a triamino-tri-s-triazine intermediate (also called 'melem', labelled as *v* in Fig. 4), when heating

goes above 360 °C [33,34]. As temperature continuously rises, polymerization yields a poly-heptazine network, assisted by hydrogen bonds and π-π stacking interactions among the units [34–37]. By a different approach, it is also possible to synthesize triazine-based frameworks, which are recently emerging as class of promising structures [31,38].

In this sense, temperature is a pivotal parameter in the synthesis of this class of materials, as different polymorphs can be obtained depending on the degree of polymerization [22,37,38]. Indeed, melem molecules first polymerize in form of non-directional 1D strands, also known as 'Liebig's melon' $[C_6N_7(NH_2)(NH)]_n$, which still contain hydrogen atoms to complete 'unbonded' amino groups [18,38]. When the condensation temperature is kept at values above 520 °C, the in-plane organization of the tri-s-triazine units improves, yielding a 2D network [22,39]. This structure, sometimes referred as 'graphitic-CN' (g-CN), consists of planes of sp² carbon and nitrogen atoms, with an ideal C/N ratio of 0.75 (but typically smaller because of local defects and boundary imperfections), connected into π-conjugated fashion. X-ray diffraction patterns (XRD) allow to better describe the crystallographic nature of the resulting PCN. In detail, the two main peaks at 2θ equal to 13.0° and 27.4° (see Fig. 5a) can be associated respectively to the (100) and the (002) planes, thus describing an intralayer spacing of 6.8 Å (d_1 in Fig. 5a) and an interlayer-stacking distance of 3.20 Å (d_2 in Fig. 5a) [22,39–41].

As for many other polymeric semiconductors [43,44], the extended conjugation, which is brought by π-symmetry, contributes to describe a band structure. In particular, it is possible to highlight some important features of PCN (Fig. 5b): (i) the wave function of the valence band is mainly derived from melem's highest occupied molecular orbitals (HOMO) levels, which in turn are a combination of p_z orbitals (perpendicular to the plane) of nitrogen atoms; (ii) the conduction band originates from the combination of both carbon- and nitrogen-centered orbitals (with a slight predominance of 2p from carbon); (iii) there exists a band gap approximately 2.7 eV (for a PCN obtained from condensation at 550 °C), which is accessible to the photons in the visible range of the solar spectrum [22,42]. Importantly, the band gap can vary with the synthesis temperature, because it may induce modifications on the
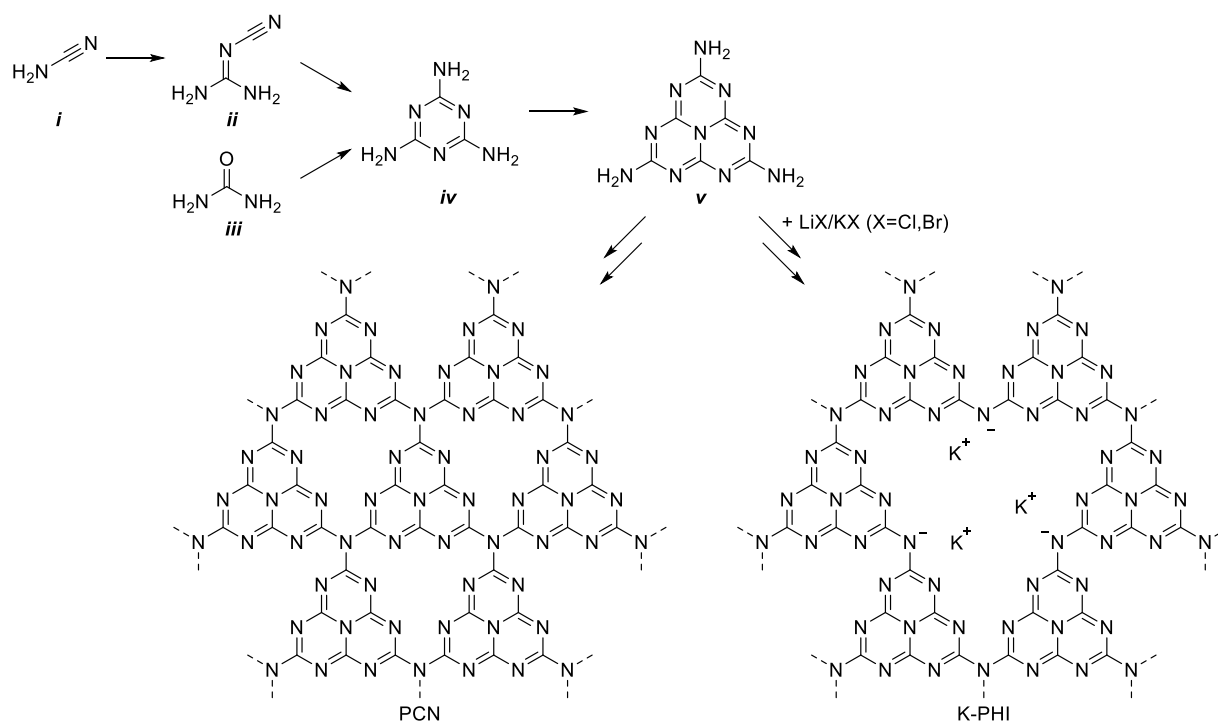

Fig. 4. Schematic representation of the polymerization process by its precursors (*i*) cyanamide, (*ii*) dicyandiamide, (*iii*) urea and (*iv*) melamine. Passing through the melem intermediate (*v*), condensation continues towards the formation of PCN or K-PHI, if salt melts are added.
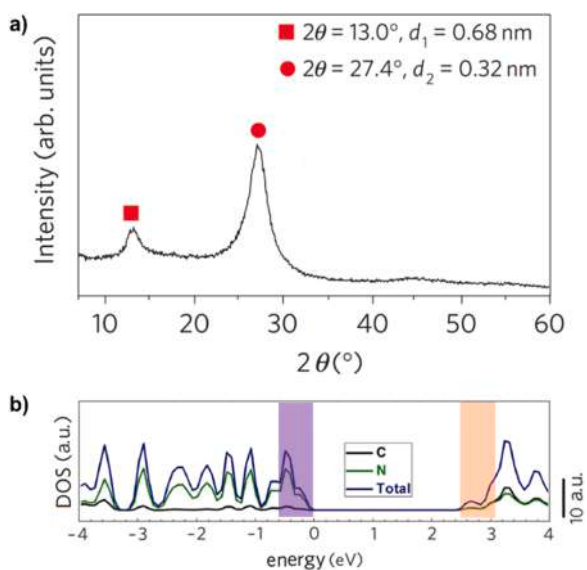
Fig. 5. (a) Experimental XRD pattern for bulk PCN (by calcination at 550 °C). Adapted with permission from ref. [39] Copyright 2005 WILEY-VCH Verlag GmbH & Co. KGaA, Weinheim. (b) Density of states (DOS) profile calculated for bulk g-CN (VB and CB are highlighted in purple and orange, in turn). Valence band edge value is set as 0 for reference. Adapted with permission from ref. [42] Copyright 2013 American Chemical Society.

materials' architecture, including deviations from the planarity [22,40, 45].

Nonetheless, not always these structural defects are detrimental to carbon nitride's properties. In 2015, Kang et al. observed that an additional heating step at 620 °C on PCN brought a disruptive amorphization of its long range-order, by cleavage of the hydrogen bonding [46]. Since the covalent C—N bonds cannot be easily broken under these operative conditions, the connectivity is retained, resulting in twisting and twinning phenomena on the melem units along the chains [46]. Moreover, the degree of amorphization increases as long as the thermal treatment is carried on [47]. Consequently, the conduction band edge is downshifted and the band gap narrows [46]. The so-called 'amorphous-CN' (am-CN) has been also characterized through electron paramagnetic resonance (EPR) spectroscopy to study spin and radical defects distribution [48,49]. In this regard, EPR experiments performed on crystalline PCN and am-CN remarked that radical species are present and evenly distributed in both the examined materials, but the less crystalline structure of the latter cuts the variety of different paramagnetic defective centers from three to one (see Fig. 6)[48]. Time-resolved EPR analysis additionally highlighted that exciting am-CN over its band gap (within the wavelength range of 355–600 nm) can produce a stable

triplet exciton that exhibits slower recombination rate and, consequently, can be efficiently exploited to drive photo-reactivity [50].

Among the other structures of PCN, we should devote particular attention also to its 'ionic' forms. Some of these crystalline materials are named 'poly(heptazine imide)s' (PHIs) and are obtained following a consecutive two-step protocol based on (i) polymerization of melem into melon chains and (ii) calcination in presence of molten salts [38,51,52]. Since melon is stable up to 650–700 °C, inorganic salts (as well as binary or ternary eutectic mixtures of these) whose melting point is below this limit can melt and form an ionic liquid matrix that deeply influences the condensation mechanism. As a result, the properties of the final material are affected, even when the salts themselves are washed away in the post-synthetic purification [38]. Compared to the PCN structure, part of the nitrogen atoms that link heptazine units within PHIs are negatively charged (as drawn in Fig. 4) with an imide behavior [52]. The lack of the 'central' heptazine not only endows the polymer of wider channels, but also represents a good coordination site for counterions, which is potassium for the typical example based on LiX/KX eutectic (X = Cl, Br) [51–53]. Protocols might include the use of electron-rich C,N-precursors, such as 5-aminotetrazole [54] and 3,5-disubstituted-1,2,4-triazole derivatives [55], but synthetic alternatives exist also for cations such as NaCl [56], KSNC [52,57], KOH and NaOH [58,59]. Interestingly, according to Krivtsov and colleagues, the use of KOH/NaOH melts reduce polycondensation temperature down to 330 °C and leads to a water-soluble photocatalyst for quasi-homogeneous applications [58, 59]. It should be additionally remarked that KSCN is used in virtue of its low decomposition temperature which brings defective terminal cyanamide groups (usually written as −NCN) to the carbon nitride layers (sometimes labelled as 'NCNCN') [60,61]. Furthermore, because of the weak ionic interactions that bind the cations (e.g., K+) to the material, it becomes possible to replace these species with other active metal centers, as we will discuss later. Other notable examples of 'ionic' structures are represented by protonated carbon nitrides. Already in 2008, Zhang et al. noted that treating PCN in strong acid (such as HCl 37 wt.%) not only kept the material intact, but also improved H$_2$ production efficiency by a factor of 2 because of higher ionic conductivity [62]. In the case of PHI, Schlomberg et al. noted that solvation water carried by K+ inside K-PHI's channels determines an offset in the piled planes, while the exchange with more weakly solvated H+ ions restores stacking faults (see Fig. 7a-f) [52]. It has been observed also for a NCNCN by Chen et al. that protonation of the terminal −N−−CN groups to −NH−CN helps reducing exciton boundary radius, thus improving charge distribution within the layers and carriers' mobility [63].

Importantly, in recent years, a great deal of research has focused on PHIs and NCNCNs because of the possibility to photochemically generate unique polaronic states in oxygen-free environment (Fig. 7g and h) [52, 64,65] which keep stable even after stopping illumination. The so-called 'Illumination-Driven Electron Accumulation in Semiconductors'

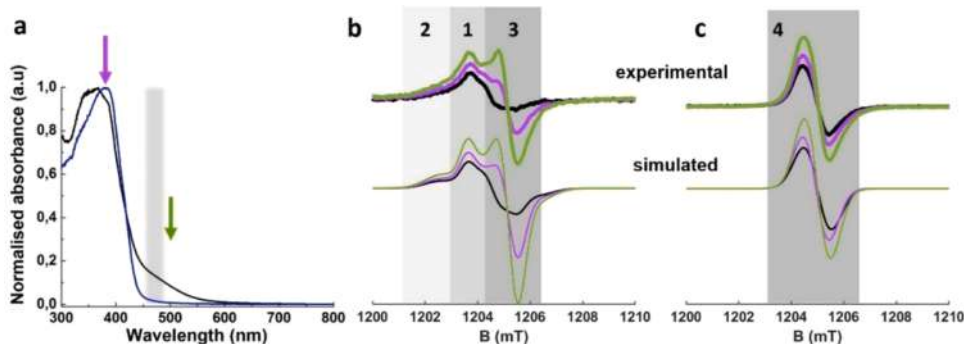**Fig. 6.** (a) Absorption profiles for crystalline PCN (black line) and am-CN (blue line). (b,c) Q-band EPR spectra on crystalline PCN (b) and am-CN (c) have been recorded after illumination below and above the materials' band gap, respectively 500 nm (green line) and 355 nm (purple line). Reprinted from ref. [48] under terms of the CC license. Copyright 2022 WILEY-VCH Verlag GmbH & Co. KGaA, Weinheim.
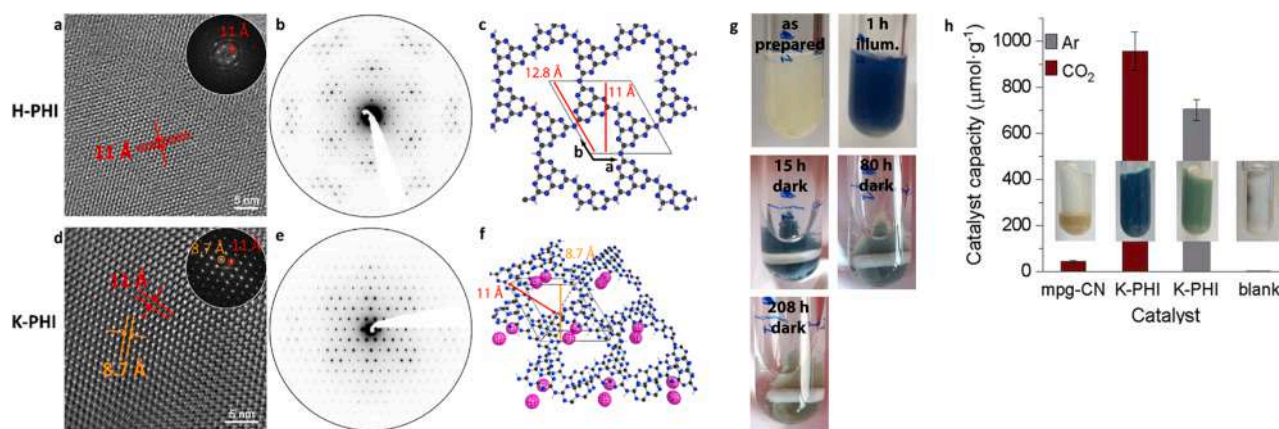
Fig. 7. (a) Transmission electron microscopy (TEM) image and (b) selected area electron diffraction (SAED) pattern of the [001] zone axis of the H-PHI given its trigonal cell (c) against 6-fold symmetry K-PHI depicted in the corresponding figures (d-f); (g) progressive fading over time (208 h) of photoreduced 'blue' H-PHI after 1 h of illumination while keeping the vessel in dark conditions. Atom color list: blue= nitrogen, dark gray= carbon, white= hydrogen, pink= potassium. Adapted from ref. [52] under terms of the CC BY license. Copyright 2022, American Chemical Society. (h) Electron capacity (expressed as $\mu mol(e^-)g^{-1}$) stored in K-PHI upon 24h-illumination. Reprinted from ref. [64] under terms of the CC BY license. Copyright 2019, The Royal Society of Chemistry.

(IDEAS) is therefore appealing for applications in dark (or 'round-the-clock') photocatalysis [15,51,57,66] and photo-chargeable devices [51, 53,67–70].

2.2. Tuning the morphology

Among the carbon nitride-based materials, the long-range ordered PCN (also 'g-CN') is the most frequently investigated allotrope in photocatalytic applications because of its robustness and stability [26]. However, this material suffers from typically low surface area, which stands around 10 m^2g^{-1} [25]. As heterogeneous catalysis relies on superficial interactions between substrates and active sites, increasing the available area may directly translate in higher performances and, eventually, better selectivity. To address this issue, several protocols have been designed to manipulate material's shape. It has to be taken into account that morphological modifications may also alter the band gap as a consequence of the creation of atom vacancies and defects (including amorphization at the layers' edges), that we will discuss in further detail in the next section.

2.2.1. Exfoliation

Exfoliation is considered as the easiest way to increase the surface area of PCNs. Unstacking the planes of PCN brings photocatalytic features as 2D material (*i.e.* fast exciton separation, higher charge carriers lifetime and presence of quantum confinement effects) [71,72] and increases the surface area, theoretically up to 2500 m^2g^{-1} [73]. As for other layered materials, delamination can be obtained by means of (i) dry thermal or (ii) wet routes. In 2012, Niu *et al.* were able to reduce the thickness of the PCN nanosheets down to 2.62 nm by applying a 'thermal oxidation' method which involves the calcination of the bulk material at 500 °C for 2 h in air [71]. Such an oxidation results in the formation of nitrogen vacancies on the surface [71]. Later on, Chen *et al.* applied a similar approach for the systematic investigation of the properties exhibited by the exfoliated materials after thermal etching [74]. The authors observed that a second condensation step at 700 °C was the most effective way to reduce the thickness down to 0.2–0.4 nm (Fig. 8b,c), as also proven by the ipsochromic shift on the absorption edge due to quantum confinement (see Fig. 8e). However, the authors also pointed out that such treatments induce buckles through intra-layer supramolecular interactions (see the zoomed area in Fig. 8c,d), which unlock n → π* transitions and extend the material's absorption range with an additional peak at approximately 500 nm (Fig. 8e) [74]. The band gap widening has been proven to be pivotal in selecting the reduction pathway of the adsorbed O_2. In detail, Guo and co-workers observed that the higher surface energy and the improved charge separation in exfoliated PCN facilitate the formation of an 1,4-endoperoxide intermediate

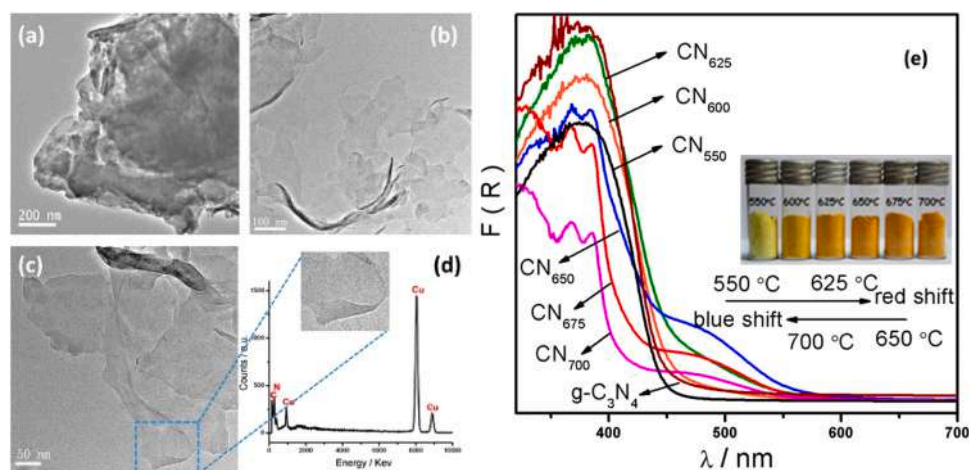**Fig. 8.** TEM images of (*a*) bulk PCN and (*b,c*) of its exfoliated sheets at 700 °C, with (*d*) energy-dispersive X-ray spectroscopy (EDS) analysis on the zoomed area, and (*e*) reflectance spectra for the materials examined. Adapted with permission ref. [74]. Copyright 2014, American Chemical Society.

(already characterized by Shiraishi *et al.* [75]) which is subsequently reduced to H_2O_2 upon two-electron transfer process [75,76]. Conversely, the electron transfer kinetics is slower on bulk PCN, therefore oxygen is preferentially reduced to $O_2^{\bullet -}$ [76].

However, thermal protocols are not always appropriate as they may compromise the stability and the nature of interfaces (*i.e.*, in composites with thermolabile substrates), several other relatively milder liquid strategies have been developed [72]. For example, exfoliation could be achieved by alkaline-promoted (aqueous NaOH solution, 0.1 M) hydrothermal protocol at a temperature as low as 90 °C, obtaining 6.5 times higher surface areas [73]. On the other hand, acidic etching has been also explored [77]. In this case, fuming H_2SO_4 is first intercalated within PCN layers at room temperature, so that when the solution is poured in water, the local heat generated by dissolution makes the stacked structure quickly expand, thus exfoliating the material [77]. Other reported protocols are based on solvothermal or sonochemical routes involving selected solvents as swelling agents [78,79]. In this sense, the solvation power is of considerable importance since the mixing enthalpy decreases rapidly in parallel with the interactions between material's layers and solvent molecules [72,78,79]. Nonetheless, solvation properties are not the only factor affecting the delamination, and other aspects need to be taken into account, such as the solvent boiling point, viscosity and molecular size [80].

2.2.2. Hard and soft templates

Besides nanosheets, increased surface area can evolve from tailored bottom-up approaches designed to modulate the final morphology. The most investigated and used technique involves the use of external templates which thereafter have to be removed without altering the carbon nitride properties. Silica nanostructures are the most popular templates and were used for the first time by Groenewolt and Antonietti in 2005 [39]. By using porosity-controlled silica monoliths soaked with molten cyanamide, PCN nanospheres with diameter of 5, 16 and 30 nm and surface area of *ca.* 100 m^2g^{-1} could be prepared [39]. The matrix was then removed with aqueous HF 5% solution [39], though nowadays the

use of 4 M NH_4HF_2 is preferred to minimize safety issues [81]. By a different approach, Goettmann and colleagues were able to obtain a mesoporous PCN framework (see Fig. 9a), with randomly connected spherical pores and improved surface area up to 440 m^2g^{-1}, by selecting an adequate ratio between cyanamide and Ludox HS40 silica nanospheres [81,82]. Casting on silica has been representing a relatively simple but effective method for templating shapes other nanospheres. Indeed, it has been possible to yield PCN nanorods within the mesoporous channels of Santa Barbara Amorphous-15 silica matrix (SBA-15, see Fig. 9b) [83–87], but also 3D cages and cubic *Ia-3d* frameworks could be obtained by exploiting structures like SBA-16 [88], KIT-6 [89–91], or FDU-12 (Fig. 9c)[86], which consist of an ordered 3D framework of nanocages mutually connected with a precise spatial periodicity. Noteworthily, nanocasts with intrinsic chirality can transfer optical activity to the templated material. Zheng *et al.* were indeed able to obtain a helical PCN (see Fig. 9d) with distinct left-handed chirality by means of a mesoporous silica mold which was templated itself around *N*-myristoyl-L-alanine [92]. Aside from silica, state-of-the-art hard--template protocols to control porosity and surface area include examples with also NaCl [93,94], anodized Al_2O_3 (AAO, etched with H_3PO_4 or NaOH, see Fig. 9e) [95–99] and $CaCO_3$ (then dissolved in HCl 2 M) [100]. Despite the excellent reproducibility of hard-templated PCNs, removing the mold *via* chemical etching introduces waste that burdens syntheses' atom economy and requires additional care during the process. A 'greener' alternative is offered by the soft agents, which are supramolecular adducts and micelles made of surfactants, amphiphilic block copolymers or ionic liquids under specific conditions of solvent polarity and temperature. In this framework, attempts with Triton X-100 and Pluronic 123 proved not ideal, as extra carbon coming from the surfactant remained incorporated during template removal by pyrolysis, affecting the final composition of the material [101–103]. Conversely, even though ionic liquids do not suffer from thermal degradation, they could interfere with the condensation mechanism, even embedding heteroatoms in the structure. Namely, BF_4^- and PF_6^- anions, respectively coming from 1-butyl-3-methylimidazolium tetrafluoroborate ([Bmim]
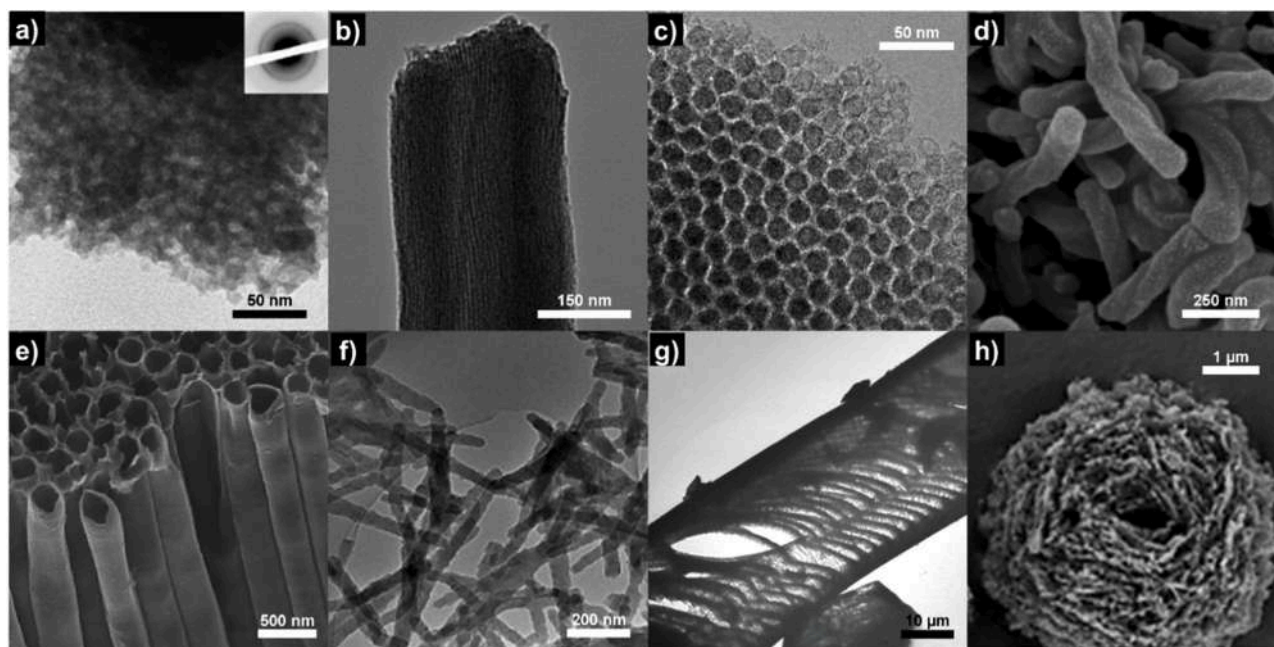

Fig. 9. TEM images for PCN templated with (a) Ludox HS40 nanospheres, (b) SBA-15 and (c) FDU-12; Scanning electron microscopy (SEM) pictures of those PCN morphology-controlled by (d) helical silica structures and (e) AAO membranes; TEM images of (f) nanobelts and (g) the nano-'accordion' and (h) SEM image of the nanoflower obtained by self-assembly techniques. Adapted with permission from, in turn, ref. [81] Copyright 2006, WILEY-VCH Verlag GmbH & Co. KGaA, Weinheim; ref. [86] Copyright 2012, The Royal Society of Chemistry; ref. [106] Copyright 2014, Elsevier Inc.; ref. [92] Copyright 2014, WILEY-VCH Verlag GmbH & Co. KGaA, Weinheim; ref. [98] Copyright 2009, American Chemical Society; ref. [107] Copyright 2012, WILEY-VCH Verlag GmbH & Co. KGaA, Weinheim; ref. [108] Copyright 2020, WILEY-VCH Verlag GmbH & Co. KGaA, Weinheim; ref. [109] Copyright 2023, Elsevier Inc.

[BF$_4$]) and 1-butyl-3-methylimidazolium hexafluorophosphate ([Bmim][PF$_6$]), are accounted of inserting B, F or P heteroatoms [104, 105].

2.2.3. Self-Assembly and template-free methods

While being extremely effective in terms of surface area output and shape-modeling reproducibility, these routes lack atom economy since the templating agent could barely be restored at the end of the synthetic protocol. Alternatively, these shapes might be achieved through strategies that rely on self-assembly phenomena among precursors.

For example, PCNs with dot-like or packed layered morphologies were obtained through the formation of complex superstructures between melamine and halogen anions coming from HCl or HBr [110]. Cyanuric chloride can be also used for low-temperature carbon nitride syntheses. Indeed, by using acetonitrile in subcritical conditions (180 °C in stainless-steel autoclave), Cui *et al.* obtained nanobelt-shaped PCN from the condensation between cyanuric chloride and melamine (see Fig. 9f)[107]. The authors remarked also a strong dependence of the material's performances on the synthetic conditions, *i.e.* material carbonization is observed if temperature exceeds 230 °C, while surface area improves after long treatments (96 h) [107]. Finally, melamine and cyanuric acid can form a supramolecular donor-acceptor adduct with stacked ordered planes, favored by strongly-directional hydrogen bonding [108]. Calcination of this aggregate generates nanosheets [111] or accordion-like (see Fig. 9g) [80,108] structures, although other morphologies are also accessible in presence of additives (e.g. oxalic acid [112] and urea [113,114]), by changing the solvent properties [115,116] or by tuning precursors' supersaturation (obtaining even flower-like shapes as Fig. 9h) [109]. Furthermore, the melamine-cyanuric acid complex offers high flexibility towards the inclusion of other precursors (albeit bearing adequate moieties for hydrogen bonding), such as caffeine [117] and creatine [118].

2.3. Engineering band gap and active sites

Band gap tuning is an important aspect in carbon nitride photocatalysis. As mentioned before, there is a clear dependence of band gap with respect to morphology and structural modifications (vacancies, doping etc.). As it is well-known from semiconductors' photophysical investigations, the presence of structural defects introduces additional electronic states within the valence and conduction band edges, which may both lower the actual band gap and serve as charge carriers' traps [12,16].

Nitrogen-rich forms of carbon nitride can be obtained either by altering the graphitization process with tailored precursors and conditions, or through post-synthetic modifications. For example, high-crystallinity mesoporous carbon nitrides with C$_3$N$_5$ [90], C$_3$N$_6$ and C$_3$N$_7$ stoichiometries [91] could be synthesized by templating tri- and tetrazoles' polymerization inside KIT-6 pores. Even though the high amount of less thermodynamically stable N−N bonds might look detrimental for material's stability, the authors demonstrated that this is retained by the thermally-induced formation of 5-member rings (see Fig. 10) at the material's edges [91]. The formation of nitrogen-rich

holey nanosheets has also been observed after thermal treatment of bulk PCN (from dicyandiamide) in NH$_3$ atmosphere [119].

Alternatively, microwave-assisted routes offer a more feasible and accessible strategy to create carbon vacancies inside PCN framework [120]. In a recent publication, Torres-Pinto *et al.* presented a systematic investigation into the features imprinted by microwaves (MW) during polymerization or post-synthetic treatments, even changing precursors [121]. According to their findings, MW-assisted polymerization produced PCNs low in nitrogen content and surface area. On the other hand, an additional post-synthetic treatment under microwaves at 500 °C helped the materials' expansion (up to 5 times), but also decreased (on average, 10% less) the amount of carbon in the structure [121]. Our group recently set up a milder protocol to generate carbon vacancies (upon loss of CO$_2$ and CO molecules) by treating melamine-derived PCN under microwave irradiation at 190 °C in presence of water [122]. Combining observations from X-ray photoelectron spectroscopy (XPS), electron nuclear double resonance (ENDOR) and solid state ^{15}N-nuclear magnetic resonance (NMR), the formation of terminal imines and triazole moieties was proposed as a structural evolution from the generated carbon vacancies [122]. It must be highlighted also that such defects play an important role in the activation of O$_2$ *via* photogenerated electrons, therefore improving oxidations. In detail, the enhanced activation is due to an uneven charge distribution on the N-rich moieties which increases the contribution of lowest unoccupied molecular orbital (LUMO) from O$_2$ in the superficial adduct between CN and O$_2$ [123].

On the other hand, several techniques have been explored to remove nitrogen atoms from the polymeric network. For example, Yu *et al.* observed that the addition of alkali (like KOH, NaOH or Ba(OH)$_2$) during urea polycondensation brings to the formation of terminal cyano groups (while losing amino functionalities) and nitrogen vacancies in the heptazine cores [124]. In addition, abstraction of nitrogen atoms may be induced by means of reducing treatments on bulk PCN, such as direct 300 W Xe lamp irradiation in presence of hydrazine [125] or thermal treatment in pure H$_2$ or Ar/H$_2$ atmosphere [126,127]. Where the structure lacks of nitrogen atoms, new carbon-carbon interactions appear, resulting in the lowering of the conduction band (see Fig. 11) [49,124].

Distributing carbon and nitrogen vacancies in a tailored space-precise pattern or gradient is of paramount importance for the formation of effective homojunctions, whereby charge carrier separation and lifetime are improved. It was demonstrated that a 1:1 mixture of melamine/cyanuric acid in presence of suitable amounts of barbituric acid led to develop heterojunctions that proved critical for enhanced photocatalytic H$_2$ evolution [128]. Since barbituric acid has hydrogen-bonding acceptor features similar to cyanuric acid, precursors' assembling is only slightly altered, but polycondensation easily yielded carbon-rich networks interfaced with non-doped carbon nitride [128]. Later, the authors improved the design by bringing together also nitrogen-rich domains when HCl is added to the supramolecular adduct mixture [129]. Noteworthily, Yang *et al.* recently implemented an analogous interface by milling and calcining in air a solid mixture of thermally polymerized melamine- and 3-amino-1,2,4-triazole-based carbon nitrides [130].
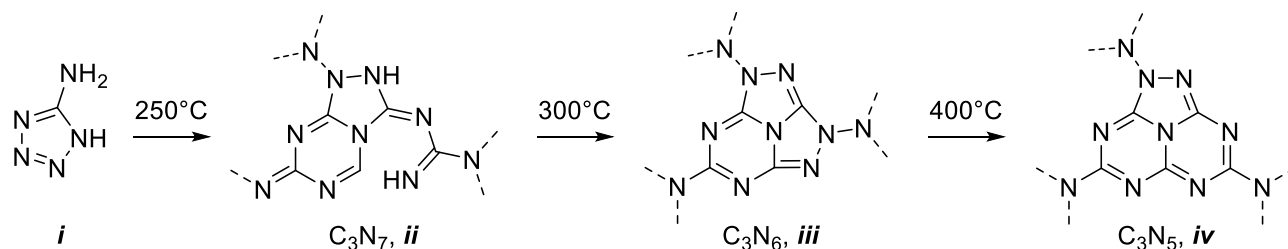

Fig. 10. Hypothetical mechanism for the formation of nitrogen-rich carbon nitrides from the pyrolysis of 5-amino-1H-tetrazole (*i*). Reprinted and adapted with permission from ref. [91]. Copyright 2019 WILEY-VCH Verlag GmbH & Co. KGaA, Weinheim.
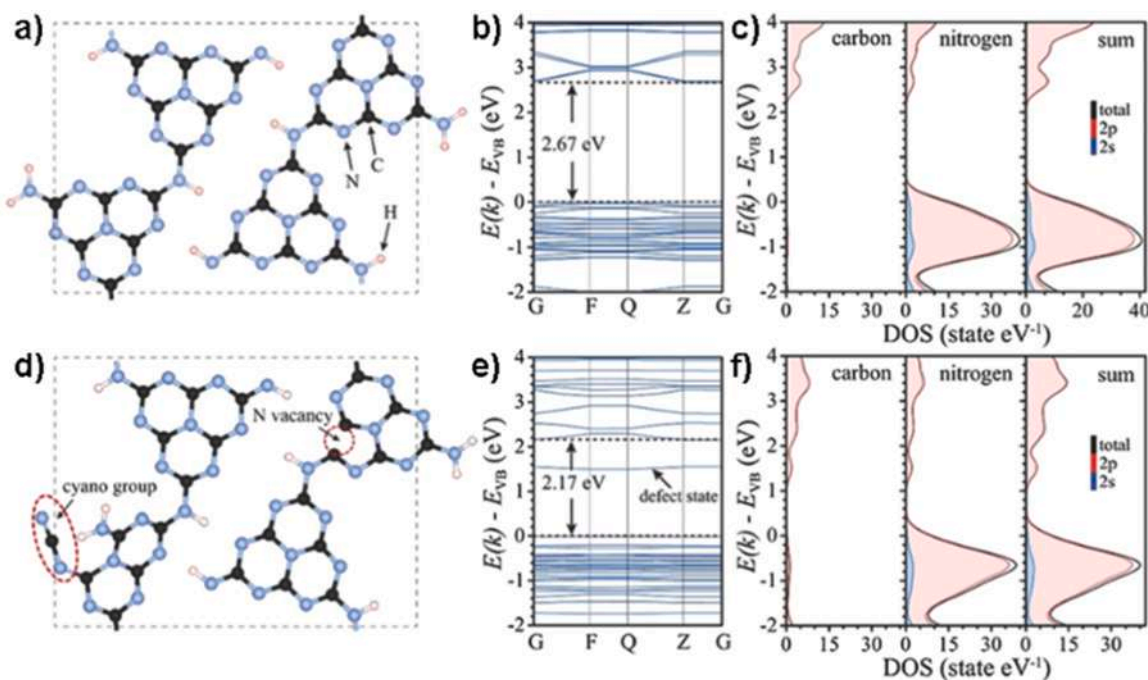
Fig. 11. Structural models, band structures and DOS respectively calculated for g-CN (a-c) and N-defective PCN (d-f). Atom color list: cyan= nitrogen, dark gray= carbon, white= hydrogen. Reprinted with permission from ref. [124]. Copyright 2017 WILEY-VCH Verlag GmbH & Co. KGaA, Weinheim.

Oxygen is another common dopant for CN structures. Oxygen-based functional groups might be purposefully introduced into the polymeric network by means of controlled oxidation protocols. The use of H_2O_2 at relatively high temperature (140 °C) and pressure leads to the substitution of sp^2-hybridized nitrogen atoms with oxygen so that the oxidized PCN displays a narrowed band gap because of new intragap states close to the CB [131]. Further details on the nature of these defects have to be linked to the oxidant's strength as well as to the protocol used. For example, diluted acid solutions cause partial etching of the PCN layers, which expose mainly −OH groups [127], while >C=O and −COOH are generated by means of stronger oxidants, such as $KMnO_4$ in acidic environment [132] or a mixture of sulfonitric acid (H_2SO_4/HNO_3 1:1 ratio) and H_2O_2 [133]. Alternatively, oxygen-rich precursors, like hexamethylolmelamine [134] or urea/cyanuric acid mixtures [135], can be used, resulting in the formation of oxadiazine fragments. Likewise, other non-metals can be effectively loaded among carbon and nitrogen atoms, imprinting their chemical features to the final material [136]. In particular, inclusion of phosphorus [105,137–139], sulfur [140,141], or boron atoms [142,143], through coordinative bonds in the polymeric network has been reported, while halides usually dope PCN *via* electrostatic interactions [144–146].

Finally, it is important also to mention the importance of metal doping, which is crucial as for tuning the optical features (*i.e.*, photosensitizing) [136,147] as for crafting catalytic sites within the frame of 'single-atom catalyst' (SAC) design [148–151]. Inspired by metalloenzymes, heterogenous SACs bridge homogenous and heterogenous catalysis while improving the effective atom utilization, which represents a great strength for those reactions catalyzed by precious metals' nanoparticles [148–152]. From the molecular point of view, carbon nitride-based materials perfectly fit as supports for metal cations since they contain 'nitrogen pots', which are coordinative sites made from heptazine's nitrogen lone pair electrons [151,153]. Complementarily, cations might be stabilized even from edge structural defects, as for the case of Ni(II) ions in MW-CN recently reported by our group [122]. As research in this field boomed in the last 10 years, a plethora of synthetic protocols have been developed, accompanied by a wide span of accessible materials. For instance, square planar 'Co$_1$-N$_4$' single active site can

be obtained from atomic layer deposition [154], but also with wet impregnation techniques using cobalt salts or complexes like $CoCl_2$ [155], Co(acac)$_2$ (acac= acetylacetonate)[93] or Co(phthalocyanine) [111]. In particular, the use of metal-phthalocyanines is sometimes preferred to the other ways, because of the planarity of the metallic complex, which guarantees better adhesion and binding to carbon nitride layers as much as intercalation among the planes [108,111,156]. However, these specifications become of minor importance when SACs are introduced into the charged PHI framework, for which ion exchange of the desired cation with the loosely bound alkali ions is sufficient [157–159]. As we will discuss with greater detail in the next section, metal cations can directly bind and activate molecular oxygen, thus improving the catalytic activity [147,157,160].

3. Aerobic oxidation reactions

The oxidation of organic compounds is one of the most common and important classes of reactions, as it increases the molecules' chemical complexity and functionality [1,3,4]. In light of Green Chemistry principles [8,9], heterogeneous photocatalysis is a convenient tool to access these transformations, because it combines the possibility to recover and recycle the solid catalyst (rule 9, 'Catalysis') with the use of light as energy source (rule 6, 'Designed for Energy Efficiency'). Among all the possible semiconductors, carbon nitrides have been emerging recently since they are versatile and cost-effective materials, and, upon tuning of the structure and properties, they can be widely applied to organic oxidations [17,30,151,161–164]. To this end, the ideal oxidant to address Green Chemistry goals in research and industry is molecular oxygen (O_2), considering its widespread availability, especially when air is directly used as oxygen source, and the lack of toxic by-products [6,7]. Indeed, O_2 is mostly entrapped into the targeted organic substrates, maximizing the atom economy (rule 2) of the transformation. Furthermore, these photocatalytic protocols are typically safe for operators and there is no actual risk of explosion while using oxygen at ambient pressure (rule 12, 'Inherently Safer Chemistry for Accident Prevention'). Further assessments on the green metrics depend on the nature of the reaction and of its reagents. This section will describe the various
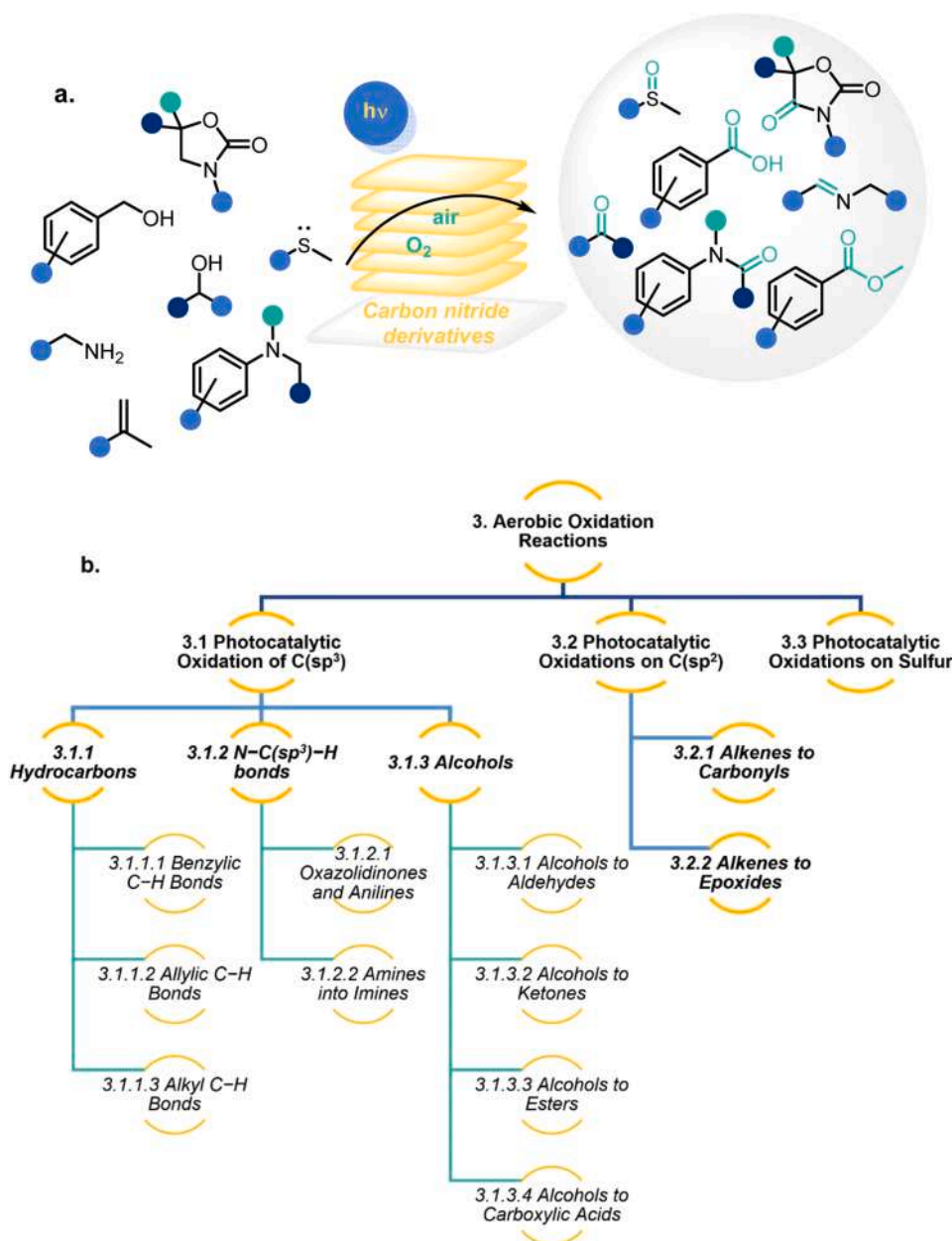
Fig. 12. (a) Graphical and (b) schematic summary of the contents of Section 3.

photocatalytic oxidation reactions catalyzed by polymeric carbon nitride derivatives relying on air or O$_2$ as oxidant (Fig. 12).

3.1. Photocatalytic oxidation of sp^3-hybridized carbon atoms

3.1.1. Photocatalytic oxidation of hydrocarbons

The oxidation of aliphatic C(sp^3)−H bonds is a core industrial technology for converting petrochemical based materials to valuable
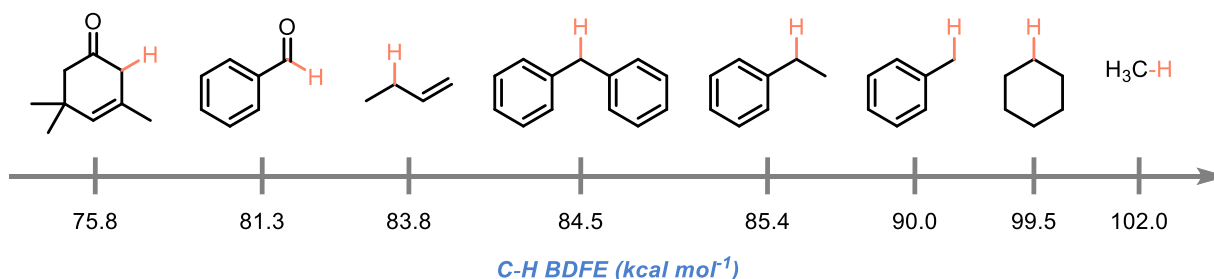

Fig. 13. Bond dissociation free energies of C—H bonds (C—H BDFEs) for some organic molecules (not in scale). Ref. [167].
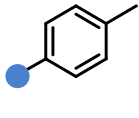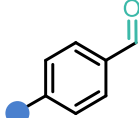
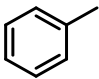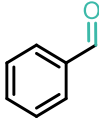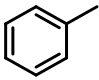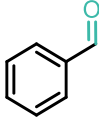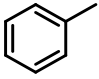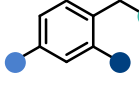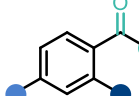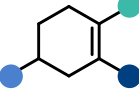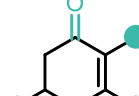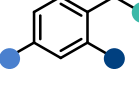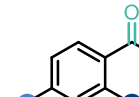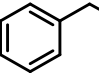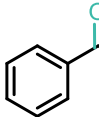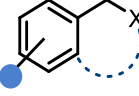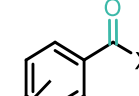chemicals [165]. However, the photocatalytic oxidation of hydrocarbon's C(sp³) to alcohols, aldehydes, or ketones with high conversion and selectivity remains a significant challenge [166], because of two main reasons: (i) the high dissociation energy of aliphatic C(sp³)−H bonds that causes low conversions especially in the case of −CH₃ groups (Fig. 13), and (ii) the increased reactivity of the oxidized products with respect to the starting material, which hampers selectivity.

3.1.1.1. Photocatalytic oxidation of benzylic C—H bonds. Toluene (C—H BDFE of 90 kcal mol⁻¹) serves well as a model substrate for the oxidation

Table 1
Examples of benzylic C(sp³)−H oxidations. [a]Thermal reaction. AQY = apparent quantum yield, FLP/FL-PCN = few-layered phosphorene/few-layered PCN, CD/PCN= carbon dots/PCN.

Entry	Catalyst	Light	Reagent	Product	Yield or Formation rate (AQY)	Sel.	Scope	Ref.
1[a]	mpg-CN	None			<3%	99%	4 ex.	[170]
2	Bi₂MoO₆/PCN	300 W Xe lamp			850.7 μmol g⁻¹h⁻¹	99%		[171]
3	BiVO₄/Ag/PCN	λ > 400 nm			150 μmol g⁻¹h⁻¹	99%	3 ex.	[172]
4	FLP/FL-PCN	Blue LED			21.9% (34%)	81%		[174]
					1–6.7 mmol g⁻¹h⁻¹	87%	8 ex.	
5	CD/PCN	λ > 400 nm			0.7–11 mmol g⁻¹h⁻¹	N.D.	5 ex.	[175]
6	NiNPs/PCN	12 W blue LED			80–98%	N.D.	35 ex.	[178]
7	Fe-PHI	200 W Hg-Xe lamp			92–98%	94.5–100%	3 ex.	[157]
8	PCN	Blue LEDs			51–94%	N.D.	35 ex.	[177]

of benzylic C—H bonds because its oxidized products, namely benzyl alcohol, benzaldehyde, benzoic acid, and benzyl benzoate, are all commercially-important intermediates for several industrial purposes [168]. Typically, the large scale production of these compounds suffers from low conversions and selectivity, and relies on homogenous precious metal-based catalysts and high reaction temperatures [168, 169].

In 2012, Li *et al.* reported for the first time the use of carbon nitride-based catalysts for the thermal oxidation of toluene and its derivatives [170]. In particular, mesoporous carbon nitride (mpg-CN) showed high selectivity towards the synthesis of the corresponding aldehydes (up to 99%), but very poor catalytic activity (conversion values spanning from 0.8 to 3.1%) at 160 °C (Entry 1 Table 1). In recent years, interest has shifted to the possibility of carrying out this oxidative process by means of more appealing photochemical approaches. Therefore, examples of toluene photo-oxidation under aerobic conditions have been reported using PCN or PCN-based composites with other inorganic [171–173] or organic [174,175] components. In general, the use of composite materials ensures efficient charge separation under photocatalytic regime, thus favoring the oxidation of the aliphatic carbons [171,173].

Fig. 14 describes the mechanism usually proposed for the photo-oxidation of toluene into benzaldehyde. First, the O_2 molecules capture the excited photoelectrons from the conduction band of the photocatalyst to generate active superoxide radical anions $O_2^{\bullet-}$, while the holes (h^+) drive the oxidation of the $C(sp^3)$−H bonds in the organic substrate to form the corresponding alkyl radical intermediates ($PhCH_2^\bullet$) and H^+. Subsequently, such radical is converted to the alkyl hydroperoxide $PhCH_2OO^\bullet$. Then, three pathways have been suggested for the synthesis of the final carbonyl compound. For example, two alkyl different hydroperoxide radicals can couple to form a $PhCH_2OOOOCH_2Ph$ intermediate and resolve into a Russel termination step [176], producing benzaldehyde, benzyl alcohol and O_2 (path 1, Fig. 14). Otherwise, $PhCH_2OO^\bullet$ may interact with H^+ to yield $PhCH_2OOH$ via an 'one electron/one proton' pathway (path 2, Fig. 14) or can react back another substrate molecule, abstracting a $H^\bullet$ and forming $PhCH_2OOH$ and $PhCH_2^\bullet$ (path 3, Fig. 14). Eventually, the dehydration of $PhCH_2OOH$ provides the desired product. Sometimes, the reaction can produce alcohols as by-products, but these would subsequently undergo an additional oxidation step to form benzaldehyde and water, improving the overall selectivity of the process [172, 174].

In 2022, da Silva *et al.* successfully performed the aerobic photocatalytic oxidation of benzylic $C(sp^3)$−H bonds, using a poly-(heptazine imide) modified with Fe single-atoms (Fe-PHI) [157]. In particular, the authors showed that the substrates could be effectively converted into the desired products with high yields and selectivity (Entry 7 Table 1). The good catalytic performances obtained using Fe-PHI are ascribable to
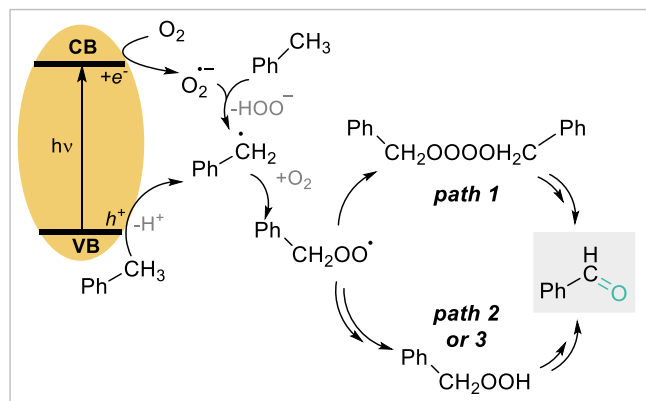
the possibility to oxidize Fe(III) single-atom sites to the active intermediates Fe(IV)=O and Fe(V)-dioxo-species, by means of the H_2O_2 generated *in situ* from the $2e^-$ photoreduction of O_2. Not only these species are very oxidative, but also the electrons stay delocalized in the PHI's π-conjugated structure to compensate the positive charge of Fe(V) species, elongating the life of excited states. However, it is important to mention that the substrates examined within this study bear substituted and dibenzylic carbon atoms, whose C–H bond dissociation energy is much lower than the one of toluene (see for reference ethylbenzene and diphenylmethane in Fig. 13). Similar considerations can be drawn for the substrate selected by Geng *et al.*, where the oxidation occurs on benzylic carbons with electron-rich atoms in the α-position (Entry 8 Table 1) [177].

Finally, it is worth mentioning even the recent efforts on the PCN-based upcycling of polystyrene as relevant example of photocatalytic aerobic oxidation of benzylic $C(sp^3)$−H bonds for industrial and environmental purposes. By means of a two-step oxidation process, the polymer can be converted into added value oxygenated molecules, mainly benzaldehyde, acetophenone or benzoic acid, with good conversions and selectivity [179,180].

3.1.1.2. Photocatalytic oxidation of allylic C−H— bonds.
Selective allylic oxidation with O_2 as the terminal oxidant is a an essential tool for organic synthesis and industrial chemistry, because introducing oxygen atoms into unsaturated hydrocarbons through aerobic oxidation allows the preparation of complex molecules from natural petroleum in a cheap way [4,181,182]. Traditional allylic oxidation requires the use of transition metal-containing catalysts and relatively harsh conditions [183]. Even under such operative conditions, the synthesis generally suffers from limited conversion and selectivity [184]. To tackle these issues, Zhang *et al.* developed a protocol for the oxidation of allylic carbons using PCN as photocatalyst in presence of HBT (1-hydroxybenzotriazole) as additive [181]. In particular, the authors studied the oxidation of cholesteryl acetate (CA) to 7-ketocholesteryl acetate (7-KOCA) (Fig. 15), which is a key step in the synthesis of vitamin D, reaching moderate yield (48%) and excellent selectivity (99%). The same protocol allows the conversion of cyclohexene into 2-cyclohexen-1-one (83% yield, 77% selectivity). Besides, phenylethylene, α-isophorone, α-pinene, and ethylbenzene were also suitable substrates, providing the corresponding oxidized derivatives with good selectivity (up to 84%) and moderate conversions (26–71%).

3.1.1.3. Photocatalytic oxidation of alkyl C—H bonds.
Catalytic oxidation of saturated $C(sp^3)$−H bonds of inexpensive and simple alkanes to give valuable chemicals is a complicated task in industrial and fine-chemical processes. This is due to the high dissociation energies associated to alkanes' $C(sp^3)$−H bond (see Fig. 13) [185]. Nevertheless, some examples showing the use of PCNs for the oxidation of alkane derivatives under aerobic conditions are available in literature. In particular, the direct synthesis of ethanol from methane and the conversion of cyclohexane into cyclohexanone have been investigated (Table 2) [175,186,187]. Conversion rates and selectivity levels were rather modest, especially for the ethanol production, where significant amounts of methanol and CO_2 were observed as by-products. In addition, only UV light or thermal activation of the catalyst drove the oxidation of hexane [187,188], calling for the development of improved catalysts and conditions.

3.1.2. Photocatalytic oxidation of N—C(sp³)—H bonds

3.1.2.1. Photocatalytic oxidation of oxazolidinones and anilines.
This section describes some representative examples of PCN-catalyzed the aerobic photo-oxidation of $C(sp^3)$−H showing a nitrogen atom in the α-position [189–191]. In this regard, an interesting example is the oxidation of oxazolidinones to afford 1,3-oxazolidine-2,4-dione
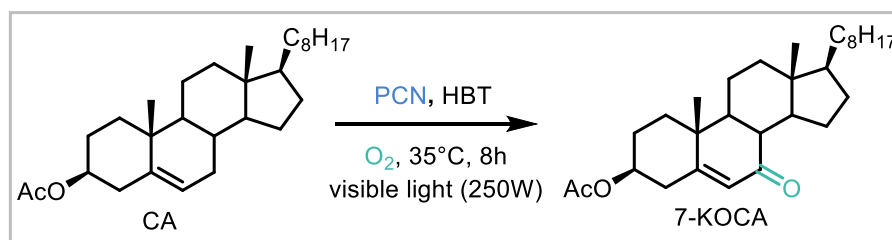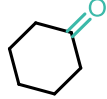

Fig. 14. Proposed reaction mechanisms for the photocatalytic oxidation of toluene using PCN. VB= valence band, CB= conduction band.
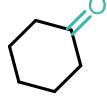
Fig. 15. Proposed reaction conditions for the oxidation of cholesteryl acetate (CA) to 7-ketocholesteryl acetate (7-KOCA). HBT =1-hydroxybenzotriazole. Ref. [181].

Table 2
Examples of oxidations of alkyl C—H bonds. PTI/PCN = polytriazine imide/PCN, GS/PCN = graphene sheet/PCN.

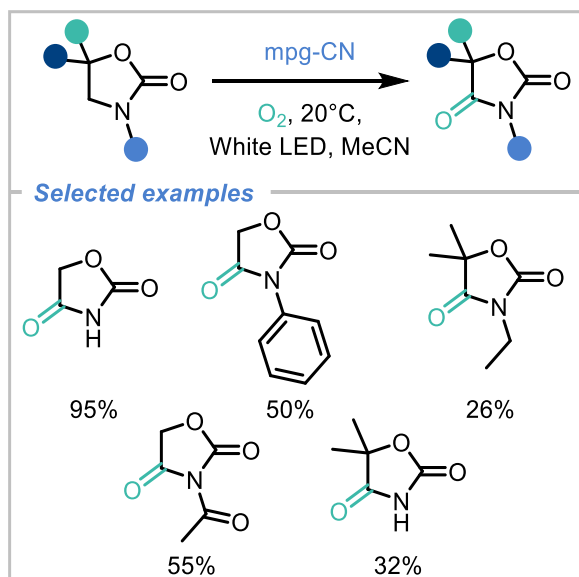| Entry	Catalyst	Light	Reagent	Product	Yield or Formation rate	Sel.	Ref.
1	*N vacant*-PCN	300 W Xe lamp	CH_4	CH_3CH_2OH	281.6 μmol g^{-1}h^{-1}	74%	[186]
2	PTI/PCN	$\lambda = $ 365–420 nm	(cyclohexane)	(cyclohexanone)	12.1%	100%	[187]
3	GS/PCN	$\lambda > 400$ nm	(cyclohexane)	(cyclohexanone)	13%	99%	[188]

Fig. 16. Use of mpg-CN for the photocatalytic oxidation of oxazolidinones. Ref. [190].

derivatives, which are relevant compounds for pharmaceutical and agrochemical industry [190]. Recently, Galushchinskiy *et al.* have shown that mpg-CN can efficiently act as heterogeneous photocatalytic system to drive this type of reactivity (Fig. 16).

By a similar approach, it is possible to perform the formylation reaction of *N,N*-disubstituted anilines. Our group recently applied PCN to this reaction, obtaining a significant pool of molecules, with yields between 24% and 86% (selected examples are reported in Fig. 17a) [192]. In comparison, other photocatalytic examples require UV light or the presence of homogeneous catalysts [193,194], so that the use of metal-free heterogeneous systems prompted by visible light is an interesting approach in potential green industrial applications. A critical step in the proposed mechanism features a single-electron transfer (labelled as 'SET (b)' in Fig. 17b) from the reagent to the photo-holes on

the excited photocatalyst in order to generate a radical cation intermediate on the nitrogen atom. As illustrated in Fig. 17b, this intermediate may be deprotonated under basic conditions, delivering an α-amino radical. Such carbon centered radical can then react with $O_2^{\bullet -}$, obtained through the reduction of O_2 *via* photoinduced SET process from the CB ('SET (a)' in Fig. 17b), eventually forming the final product.

3.1.2.2. Photocatalytic oxidation of amines into imines. Imines are important precursors in organic chemistry for many synthetic purposes, which include bioactive nitrogen-containing heterocyclic compounds, agrochemicals, organic polymers, and drug delivery vectors [195–199]. Visible light photocatalysis by mpg-CN under aerobic conditions proved promising, with yields ranging between 50 and 99% and a scope of 19 entries. However, some disadvantages such as relatively low surface area, inefficient charge transfer/separation, and large reaction energy barrier required the use of relatively unfavorable conditions such as high oxygen pressures [161,162,200]. To overcome such limitations, porous few-layer PCN [80], mpg-CN in flow reactors [201], cyano-decorated PCN nanosheets [202], perylene-3,4,9,10-tetracarboxylic dianhydride/PCN [203], PCN/UiO-66-NH₂ (in which UiO-66-NH₂ defines a NH₂-mediated zirconium-based metal-organic framework) [204], Fe (bpy)₃/npg-CN ('npg' = 'nanoporous') [205], CdS@PCN [206], PCN/Bi₂WO₆ [207] and AuNPs/PCN [208] were investigated. The higher complexity of these catalysts allows to operate under milder conditions, such as room temperature, low O_2 pressures, or even air. A generally accepted mechanism for this conversion is illustrated in Fig. 18. The first step is the loss of an electron by the amine through oxidation by a photogenerated hole, resulting in a radical cation intermediate; meanwhile, the photogenerated electron reduces O_2 to the radical anion superoxide $O_2^{\bullet -}$ [207]. In a third step, the radical cation combines with $O_2^{\bullet -}$ to produce a NH-imine and H_2O_2. Finally, the NH-imine undergoes a nucleophilic attack by another amine molecule, resulting in the formation of an intermediate that releases ammonia and produce the benzyl imine. Variations to this general mechanism were adopted by various groups. For example, zinc porphyrin polymer (ZnP PCN) and cerium single-atom PCN seem to favor $^1O_2$ as active oxygen species, and the formation of benzaldehyde as intermediate [147,160].
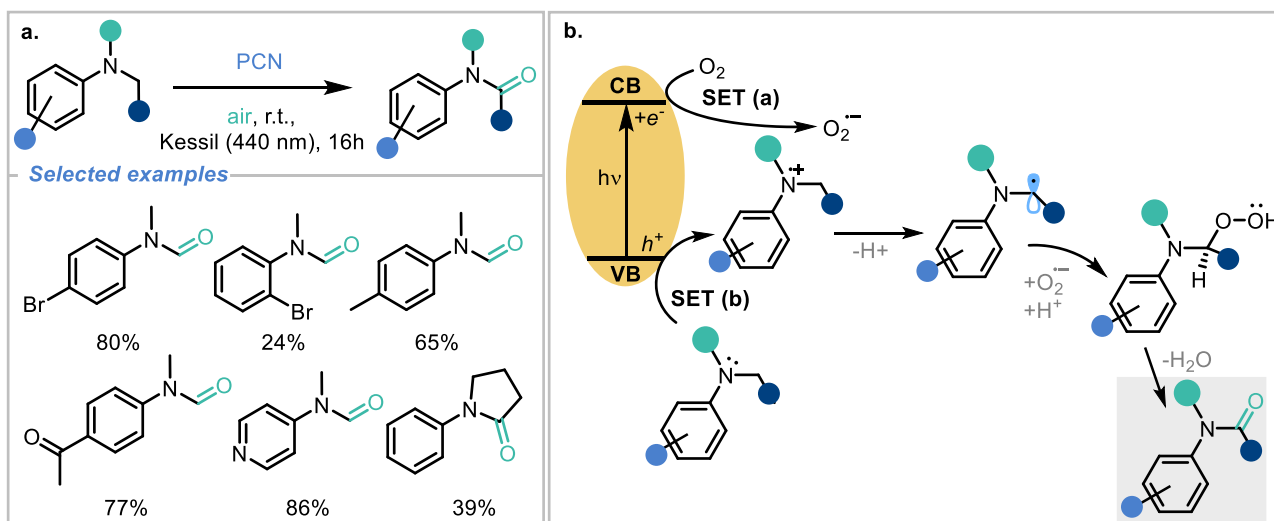
Fig. 17. (a) Oxidative formylation of amines, including the yields of some examples from the scope, and (b) the corresponding proposed reaction mechanism. VB= valence band, CB= conduction band, SET = single-electron transfer. Ref. [192].
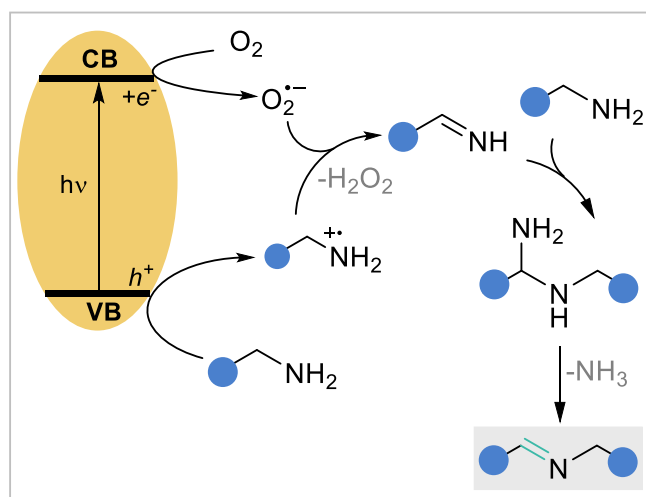

Fig. 18. General mechanism for amine-to-imine oxidation. VB= valence band, CB= conduction band. Ref. [207].

Fig. 19. Proposed mechanism for oxidation of primary alcohols to aldehydes. VB= valence band, CB= conduction band, PCET = proton-coupled electron transfer.

3.1.3. Photocatalytic oxidation of alcohols

3.1.3.1. Photocatalytic oxidation of alcohols to aldehydes. The partial aerobic photooxidation of alcohols to carbonyl compounds with carbon nitride was vastly investigated in the last decade [209], and recently reviewed by Savateev [210]. The reason of this large interest relies on the simplicity of the synthesis that makes it an ideal model reaction for photocatalyst development. Moreover, it has a large applicability in laboratory and in commercial procedures as well as in industrial processes [211–213]. The transformation however suffers from low selectivity in the case of electron-rich molecules and substrates bearing multiple functional groups [214]. Benzyl alcohol is often used as a model substrate, with O_2 as an electron acceptor (Fig. 19) and various structurally- or chemically-modified PCN have been successfully used [175,215–228]. The general mechanism, schematized in Fig. 19, begins with the reduction of O_2 to superoxide radical anion ($O_2^{\bullet-}$) by the photoexcited electrons. Subsequently, $O_2^{\bullet-}$ can take a proton from the alcohol to yield $^\bullet OOH$ and the corresponding alkoxide anion intermediate (path 1 in Fig. 19), which is then oxidized by the photo-holes to an oxygen-centered radical. Alternatively, the alcohol may also undergo a single proton-coupled electron transfer (PCET), in which it

simultaneously gives a proton to $O_2^{\bullet-}$ and an electron to the photo-holes, directly giving the oxygen-centered radical (path 2, Fig. 19). The abstraction of $H^\bullet$ from this intermediate by means of $^\bullet OOH$ closes the catalytic cycle, producing H_2O_2 and the desired carbonyl compound.

Among all the possible strategies to prevent overoxidation of benzylic alcohols to the corresponding carboxylic acids, flow reactors offer a simple and scalable solution that allow to finely control residence and irradiation time to optimize conversion and selectivity [201]. In this framework, two possible implementations have been suggested by Reisner and co-workers in 2020 [201] and, later, by Giusto and colleagues [229]. In the first example, mpg-CN was immobilized inside the channels of a microfluidic reactor in a packed-column fashion while the precursor was pushed through with a gas-liquid segmented flow pattern (which is the regular succession of reaction matrix and air bubbles) [201]. Using 1-naphthalenemethanol as model substrate, the authors remarked a huge difference in conversion (80% for the flow reactor against 39% of the batch) over 90 min and, even increasing the reaction time of the batch reaction to equalize the conversion, the selectivity dropped [201]. Alternatively, Giusto and co-workers deposited mpg-CN as thin films on the tubing walls [229]. By generating $^1O_2$ as reactive

oxygen species (which is milder than $O_2^{\bullet-}$ or $^{\bullet}OH$), the set-up allowed to isolate benzaldehyde with 96% yield (against 53% of the analogous batch process). Since pristine PCN and its derivatives possess poor yield for $^1O_2$ [230–232], the better performances of this material are probably due to higher surface area/volume ratio in the microchannels combined to the absence of voids in the structure of the thin film that suppresses the non-radiative recombination of triplet excited states [229]. Similar photophysical concepts served to the authors also to explain why instead the batch reactor was useful to yield carboxylic acids, as we will further in section 3.1.3.4.

Finally, most of the examples report benzylic substrates while just a small number of examples with aliphatic alcohols can be found [75], the reason being the stabilization effect of the aromatic towards the high-energy intermediates.

3.1.3.2. Photocatalytic oxidation of alcohols to ketones. Ketones are also possible products of the alcohol oxidation, and several examples are available [175,216,217,219,222,224]. They are usually obtained in the same conditions of the aldehydes but using secondary alcohols as substrates. Unlike aldehydes, ketones do not possess labile C—H bonds next to the carbonyl moiety, resulting in the formation of more stable ketyl radicals and an overall higher selectivity can be found [51]. However, the oxidation of aliphatic secondary alcohols to the relative ketones typically occurs with low yields (11–12 %) [175,219,224]. Improved activity (yields up to 36–55%) was obtained in acidic conditions [224].

3.1.3.3. Photocatalytic oxidation of alcohols to esters. When the photo-oxidation of benzyl alcohols is carried out in the presence of an aliphatic alcohol, such as methanol, methyl benzoates could be obtained [233–235]. For example, protonated PCN showed very high yields and selectivity for the synthesis of methyl benzoates (77–100% yield, 9 examples) [234]. Good performances were also observed with a Pd-decorated carbon nitride [235]. Conversely, interfacing PCN with $BiVO_4$ was reported to be not as selective as the previous examples (although in similar operating conditions), giving higher selectivity for acetals, but also producing benzaldehyde and benzyl benzoate (Fig. 20). The presence of these by-products can be explained through a deeper investigation on the mechanism usually proposed for this reaction: as common first step, the aldehyde is obtained as first intermediate and this can react with methanol to form a hemiacetal, which is further oxidized to the corresponding ester. However, after the hemiacetal is formed, an additional substitution reaction with another methanol molecule can generate a dimethyl acetal, halting the oxidation process [236].

3.1.3.4. Photocatalytic oxidation of alcohols to carboxylic acids. Benzoic acids are generally obtained as side products of the aerobic oxidation of benzylic alcohols, as the C–H bond in the newly-formed aldehydes is relatively more labile (81.3 kcal mol^{-1}) and can be further oxidized. The main responsible of this side reaction are the $^{\bullet}OH$ radicals given by the homolytic cleavage of H_2O_2, which is a by-product of the benzaldehyde synthesis (Fig. 19). Albeit generally considered as an undesired by-product, some groups purposely isolated the acid with high selectivity (Fig. 21a). For example, Mazzanti et al. deposited thin films of carbon nitride via chemical vapor deposition on the walls of the batch reaction

vessel. By mechanistic investigations, the authors proved the importance of the number and the uniformity of the deposited layers. In particular, not only the absence of voids in the PCN's structure eases the formation of $^1O_2$ (which is the actual ROS), but also having thicker deposits leads to a slower reaction kinetics (due to the higher rate of exciton recombination events) that favors the selective formation of carboxylic acids instead of aldehydes [229]. Another synthetic path is focused on the oxidative cleavage of the C—C bond in symmetric α-hydroxy ketones catalyzed by mpg-CN, that selectively produce the corresponding carboxylic acids (49–75% yield, 14 examples, Fig. 21b) [237]. However, the proposed synthetic strategy requires relative high temperatures (100 °C) and has moderate yields.

3.2. Photocatalytic oxidations on sp²-hybridized carbon atoms

3.2.1. Photocatalytic oxidation of alkenes to carbonyls trough oxidative cleavage of double bonds

Another common reaction in organic chemistry is the oxidative cleavage of alkenes into carbonyls (aldehydes and ketones) and carboxylic acids [238]. Classical industrial protocols for alkenes' oxidative cleavage employ O_3 as the oxidant, which suffers from high costs, significant energy demands and serious safety issues [239]. Zhang et al., reported a method for the oxidative cleavage of a large scope of alkenes using polymeric carbon nitride as catalyst and N-hydroxy succinimide (NHS) as additive (39–81% yields, 29 examples) [240]. However, atom economy guidelines discourage the use of additives [8,9]. Alternatively, tubular carbon nitride was recently exploited to achieve good results for C=C cleavage to obtain aldehydes and ketones (59–83% yields, 24 examples) without additives [241]. Compared to the 'simple' PCN, the ultrathin walls of tubular carbon nitride increase the number of active sites and the light scattering, enhancing the material's photocatalytic activity [241]. These features enhance the formation of $^{\bullet}OH$ and OH^{-} via hydrogen atom transfer between $O_2^{\bullet-}$ and water (path 2, Fig. 22), avoiding the use of other radical promoters, like NHS, and offering an alternative pathway to the [2+2] cycloaddition (path 1, Fig. 22). In both cases, the coupling between alkene's radical cation and the ROS yields a dioxetane intermediate, which leads to the final product by ring cleavage (Fig. 22).

The role of singlet oxygen was investigated for allyl and diene oxidations [242]. In this regard, oxidized carbon nitrides were proved efficient to oxidize a large number of unsaturated compounds, including allyl benzene and α-methyl styrene [242]. In most of the cases, however, the reaction shows low selectivity, and a mixture of products is obtained. As matter of fact, even if $^1O_2$ is considered to be the main active species via Diels-Alder or ene reaction with the substrates, the formation of dioxetane intermediates has been postulated to justify some of the observed by-products, raising questions on the truly active species [242]. Deeper studies will have to reveal the in-depth mechanism and the influence of active oxygen species on the oxidation of unsaturated carbons.

3.2.2. Photocatalytic oxidation of alkenes to epoxides

Epoxides are particularly interesting compounds, since they are widely used in organic syntheses for pharmaceutical industries,
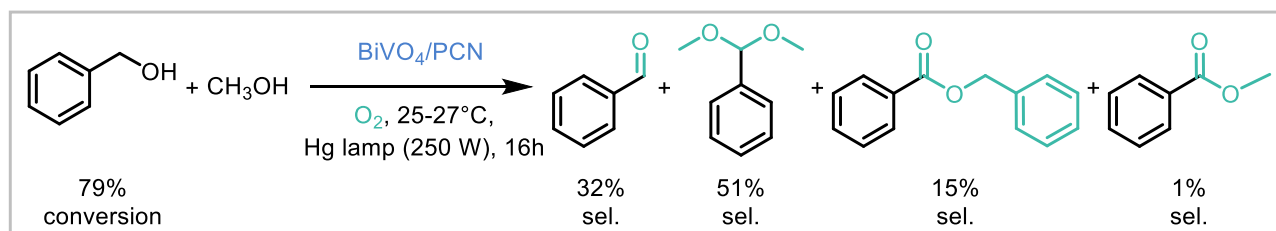
Fig. 20. Reaction conditions proposed by Samanta et al., with selectivity values for the various by-products. Ref [233].
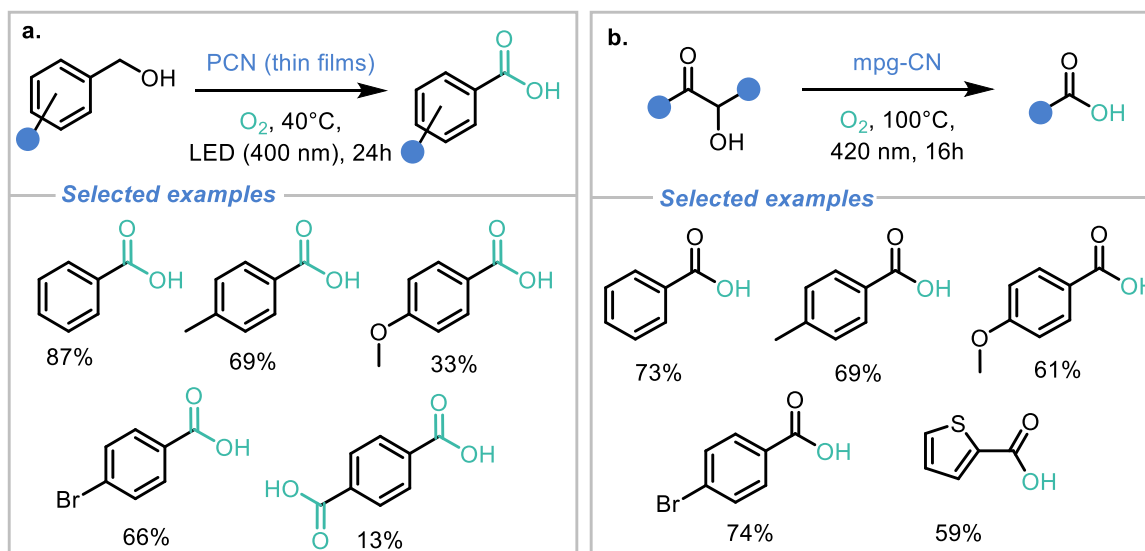
Fig. 21. (a) Oxidation of alcohols to acids. Ref. [229]. (b) Oxidative cleavage of carbon-carbon bond of α-hydroxy ketones. Ref. [237].
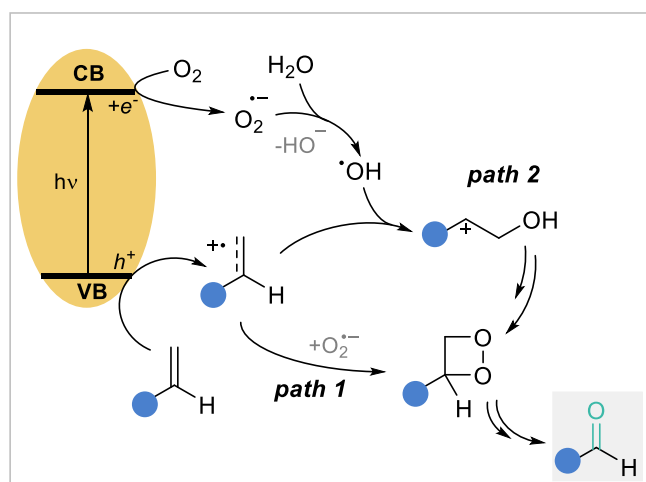

Fig. 22. Proposed mechanism for photocatalytic oxidation of alkenes to aldehydes with tubular carbon nitride trough oxidative cleavage of the double bond. VB= valence band, CB= conduction band. Ref. [241].

materials and life sciences [243]. The mesoporous carbon nitrides used were functionalized with metal complexes or nanoparticles, as reported in Table 3 [178,244]. The mechanism still needs to be further investigated, however it probably involves the presence of dioxetane intermediate [178], as described in the previous section. Interestingly, the presence of the metal in the catalyst seems to be essential to oxidize the double bond selectively to epoxide rather than to carboxylic group [244].

3.3. Photocatalytic oxidations on sulfur

Sulfoxides, because of their chiral electron pair, are extremely important for preparing biologically active molecules [245]. The classical method to generate sulfoxides is through the oxidation of sulfides, that generally requires strong oxidants [246]. For this reason, the photocatalytic oxidation of sulfides using oxygen as the oxidant and carbon nitride derivatives as photocatalysts has been attracting growing interest in recent years, as summarized in Table 4 [230–232,247–250]. The selective formation of sulfoxide makes use of $^1O_2$ [232,251,252], despite in many cases the superoxide radical is accounted as main active species in the oxidation [247,248]. $^1O_2$ shows higher selectivity than $O_2^{\bullet-}$ for sulfides oxidation because of its milder behavior that does not prompt the formation of more aggressive ROS species that can potentially overoxidized sulfoxides to sulfones. To avoid this, usually the persulfoxide diradical or dipolar intermediates are stabilized with an alcohol (Fig. 23) [232,247,248].

The most reliable mechanism can be generalized as in Fig. 23. The attack of the active oxygen species to the sulfur atom, and the consequent formation of the persulfoxide intermediate, is a commonly recognized step, while the final step may vary according to different conditions: (a) in case $^1O_2$ is the only active species, no further oxidations are possible, the persulfoxide is stabilized by the resonance between its zwitterionic and diradical structures and it most likely reacts with a second sulfide molecule to obtain two sulfoxide molecules [251]; differently, when an alcohol is present, it could (b) stabilize the persulfoxide through hydrogen-bonding interactions, avoiding further oxidation due to superoxide, and generating an intermediate that reacts with a second sulfide molecule, affording the final product, or (c) the alcohol reacts directly with the persulfoxide generating water and the sulfoxide [247].

In alternative to this mechanism, the oxygen radical species ($O_2^{\bullet-}$) may start a radical pathway reaction with isobutyraldehyde, when the

Table 3
Examples oxidation of alkenes to epoxides. Co-Sal = Co(^{tBu}Salophen)/mpg-CN.

Entry	Catalyst	Light	Reagent	Product	Yield	Scope	Ref.
1	Co-Sal/mpg-CN	450 nm LED			33–99%	20 ex.	[244]
2	NiNPs/PCN	12 W blue LED			53–89%	15 ex.	[178]

Table 4

Examples of sulfur oxidations. [a]Aldehyde as additive; the reaction scope includes an additional example of formation of disulfones from disulfide species (50% yield, 77% selectivity). AQY = apparent quantum yield, BPCN = heptazine-based polymer/PCN.

Entry	Catalyst	Light	Reagent	Product	Yield (AQY)	Sel.	Scope	Ref.
1	PCN	50 W Xe lamp			6–51%	10–67%	8 ex.	[249]
2[a]	mpg-CN	150 W Hg lamp			79–100%	77–99%	8 ex.	[250]
3	Oxidized PCN	50 W Xe lamp			97–99%	98–99%	8 ex.	[232]
4	CdS/PCN	White LED			6–86%	99–100%	5 ex.	[248]
5	fullerene/PCN	$\lambda > 400$ nm			69–100%	95–100%	12 ex.	[249]
6	CuN$_3$/PCN	$\lambda > 420$ nm			99%	99%		[231]
7	K-PHI	$\lambda =$ 465 nm			61–98%	88–98%	12 ex.	
					25–81%	25–81%	9 ex.	[230]
8	BPCN	$\lambda =$ 450 nm			traces-96% (5.72%)	>99%	7 ex.	[247]

latter is present in high quantity as additive, thus generating peroxide radicals and peracids, which become the main responsible of the oxidation of sulfides. In absence of the aldehyde the reaction proceeds in the usual pathway with the direct reaction between $O_2^{\bullet -}$ and sulfoxide but in very low yields (8%) [250]. Pristine PCN was studied by Wang *et al.* in absence of alcohol, the results indicate low selectivity towards the sulfoxides, by favoring $^{\bullet}$OH generation that leads to overoxidation and the formation of other species [232]. In other examples, single atom (Cu, Fe) carbon nitride catalysts showed selective production of $^1O_2$, ensuring high conversion and high selectivity without any additive [230–232]. The structure of these materials enhances the presence of triplet excitons that are necessary for the formation of singlet oxygen and simultaneously suppress other ROS generation. In these terms, they can be considered the ideal catalysts for sulfoxide synthesis. As a variation of the this reaction, Markushyna *et al.* exploited the peculiar properties of K-PHI to synthetize sulfonyl amides and sulfonyl chloride,

from S-arylthioacetates under 465 nm irradiation (Entry 7 Table 4) [230]. K-PHI has a high oxidation potential and is able to form $^1O_2$, both these characteristics are fundamental for these reactions.

4. Conclusions and Future Perspectives

Carbon nitride and its derivatives are versatile and cost-effective metal-free materials, that have been largely employed as photocatalytic scaffolds to drive the oxidation of organic substrates to valuable products in presence of molecular oxygen. As a matter of fact, it has been shown that, upon visible light absorption, a PCN-based photocatalyst may reach a suitable potential energy, thus becoming able to trigger the oxidation of suitable substrates and/or form reactive oxygen species from O$_2$. In this way, in recent years, it has been possible to develop a number of heterogeneous photocatalytic protocols for the sustainable production of organic molecules of industrial interest.
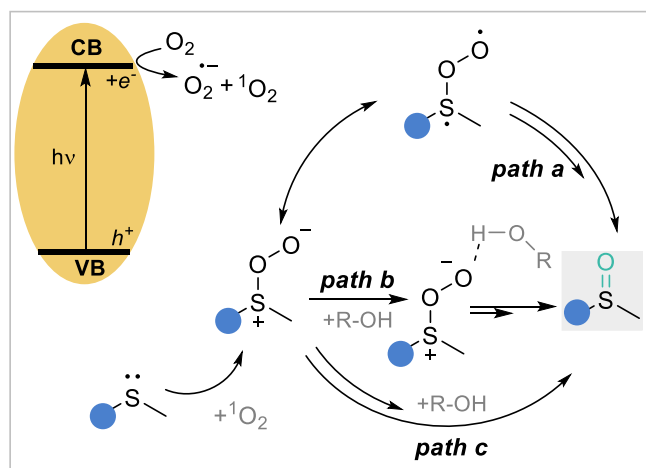
Fig. 23. Proposed mechanism for oxidations on sulfur. VB= valence band, CB= conduction band.

However, several unexplored challenges and opportunities remain unaddressed in this research field. As an example, many of these photocatalytic transformations suffer from low selectivity levels because of the formation of numerous by-products under the reaction conditions. This is primarily due to the production, under the photocatalytic conditions, of many different reactive oxygen species that may react with the organic substrate through several mechanistic pathways. Therefore, it becomes very important to design and develop novel photo-active PCN-based materials able to selectively produce specific oxygen-containing species in order to drive more controlled reaction mechanisms. In this direction, post-synthetic modifications of the materials may be effectively used to modify and tune both the morphology and physicochemical features of the photocatalysts, and consequently the outcomes of the overall processes. In addition, a great synthetic challenge is the development of novel photocatalytic protocols for the efficient and selective aerobic oxidation of aliphatic $C(sp^3)-H$ bonds (for instance within simple hydrocarbons). These are difficult reactions because of the high dissociation energy associated to these chemical bonds and the presence of many similar chemical groups within the substrates. We therefore expect that those imminent investigations on such research topics will contribute to determine the future directions in the direct oxidation of organic compounds, hence providing new photocatalytic solutions for both academia and industry.

Declaration of Competing Interest

The authors declare that they have no known competing financial interests or personal relationships that could have appeared to influence the work reported in this paper.

Acknowledgments

References

[1] F. Cavani, J.H. Teles, Sustainability in catalytic oxidation: an alternative approach or a structural evolution? ChemSusChem 2 (2009) 508–534, https://doi.org/10.1002/cssc.200900020.

[2] M. Baumann, I.R. Baxendale, An overview of the synthetic routes to the best selling drugs containing 6-membered heterocycles, Beilstein J. Org. Chem. 9 (2013) 2265–2319, https://doi.org/10.3762/bjoc.9.265.

[3] T. Newhouse, P.S. Baran, If C−H bonds could talk: selective C−H bond oxidation, Angew. Chem. Int. Ed. 50 (2011) 3362–3374, https://doi.org/10.1002/anie.201006368.

[4] C.-Y. Zheng, J.-M. Yue, Allylic hydroxylation of enones useful for the functionalization of relevant drugs and natural products, Nat. Commun. 14 (2023) 2399, https://doi.org/10.1038/s41467-023-38154-9.

[5] J. Genovino, D. Sames, L.G. Hamann, B.B. Touré, Accessing drug metabolites via transition-metal catalyzed C−H oxidation: the liver as synthetic inspiration, Angew. Chem. Int. Ed. 55 (2016) 14218–14238, https://doi.org/10.1002/anie.201602644.

[6] F. Cavani, Catalytic selective oxidation: the forefront in the challenge for a more sustainable chemical industry, Catal. Today 157 (2010) 8–15, https://doi.org/10.1016/j.cattod.2010.02.072.

[7] D.J.C. Constable, P.J. Dunn, J.D. Hayler, G.R. Humphrey, J.L. Leazer Jr., R. J. Linderman, K. Lorenz, J. Manley, B.A. Pearlman, A. Wells, A. Zaks, T.Y. Zhang, Key green chemistry research areas—A perspective from pharmaceutical manufacturers, Green Chem. 9 (2007) 411–420, https://doi.org/10.1039/B703488C.

[8] P.T. Anastas, J.C. Warner, J.C. Warner, Green Chemistry: Theory and Practice, 1. Paperback, Oxford University Press, Oxford, 2000.

[9] Handbook of Green Chemistry and Technology, J.H. Clark, D. Macquarrie, eds., 1st ed., Wiley, 2002 https://doi.org/10.1002/9780470988305.

[10] G. Sportelli, T. Boselli, S. Protti, N. Serpone, D. Ravelli, Photovoltaic materials as heterogeneous photocatalysts: a golden opportunity for sustainable organic syntheses, Sol. RRL 7 (2023), 2201008, https://doi.org/10.1002/solr.202201008.

[11] H. Kisch, Semiconductor photocatalysis for chemoselective radical coupling reactions, Acc. Chem. Res. 50 (2017) 1002–1010, https://doi.org/10.1021/acs.accounts.7b00023.

[12] H. Kisch, Semiconductor photocatalysis-mechanistic and synthetic aspects, Angew. Chem. Int. Ed. 52 (2013) 812–847, https://doi.org/10.1002/anie.201201200.

[13] W.Y. Teoh, J.A. Scott, R. Amal, Progress in heterogeneous photocatalysis: from classical radical chemistry to engineering nanomaterials and solar reactors, J. Phys. Chem. Lett. 3 (2012) 629–639, https://doi.org/10.1021/jz3000646.

[14] A. Savateev, N.V. Tarakina, V. Strauss, T. Hussain, K. Brummelhuis, J.M. Sánchez Vadillo, Y. Markushyna, S. Mazzanti, A.P. Tyutyunnik, R. Walczak, M. Oschatz, D. M. Guldi, A. Karton, M. Antonietti, Potassium Poly(Heptazine Imide): transition metal-free solid-state triplet sensitizer in cascade energy transfer and [3+2]-cycloadditions, Angew. Chem. Int. Ed. 59 (2020) 15061–15068, https://doi.org/10.1002/anie.202004747.

[15] S. Mazzanti, A. Savateev, Emerging concepts in carbon nitride organic photocatalysis, Chempluschem 85 (2020) 2499–2517, https://doi.org/10.1002/cplu.202000606.

[16] Heterogeneous Photocatalysis: From Fundamentals to Applications in Energy Conversion and Depollution, J. Strunk, ed., 1st ed., Wiley, 2021 https://doi.org/10.1002/9783527815296.

[17] C. Rosso, G. Filippini, A. Criado, M. Melchionna, P. Fornasiero, M. Prato, Metal-free photocatalysis: two-dimensional nanomaterial connection toward advanced organic synthesis, ACS Nano 15 (2021) 3621–3630, https://doi.org/10.1021/acsnano.1c00627.

[18] J. Liebig, Ueber mellon und mellonverbindungen, Justus Liebigs Ann. Chem. 50 (1844) 337–363, https://doi.org/10.1002/jlac.18440500302.

[19] L. Pauling, J.H. Sturdivant, The structure of cyameluric acid, hydromelonic acid and related substances, Proc. Natl. Acad. Sci. 23 (1937) 615–620, https://doi.org/10.1073/pnas.23.12.615.

[20] A.Y. Liu, M.L. Cohen, Prediction of new low compressibility solids, Science 245 (1989) 841–842, https://doi.org/10.1126/science.245.4920.841.

[21] C.E. Redemann, H.J. Lucas, Some derivatives of cyameluric acid and probable structures of melam, melem and melon, J. Am. Chem. Soc. 62 (1940) 842–846, https://doi.org/10.1021/ja01861a038.

[22] X. Wang, K. Maeda, A. Thomas, K. Takanabe, G. Xin, J.M. Carlsson, K. Domen, M. Antonietti, A metal-free polymeric photocatalyst for hydrogen production from water under visible light, Nature Mater 8 (2009) 76–80, https://doi.org/10.1038/nmat2317.

[23] K. Maeda, X. Wang, Y. Nishihara, D. Lu, M. Antonietti, K. Domen, Photocatalytic activities of graphitic carbon nitride powder for water reduction and oxidation under visible light, J. Phys. Chem. 113 (2009) 4940–4947, https://doi.org/10.1021/jp809119m.

[24] G. Zhang, G. Li, T. Heil, S. Zafeiratos, F. Lai, A. Savateev, M. Antonietti, X. Wang, Tailoring the grain boundary chemistry of polymeric carbon nitride for enhanced solar hydrogen production and CO2 reduction, Angew. Chem. Int. Ed. 58 (2019) 3433–3437, https://doi.org/10.1002/anie.201811938.

[25] S. Cao, J. Low, J. Yu, M. Jaroniec, Polymeric photocatalysts based on graphitic carbon nitride, Adv. Mater. 27 (2015) 2150–2176, https://doi.org/10.1002/adma.201500033.

[26] W.-J. Ong, L.-L. Tan, Y.H. Ng, S.-T. Yong, S.-P. Chai, Graphitic Carbon Nitride (g-C 3N 4)-based photocatalysts for artificial photosynthesis and environmental remediation: are we a step closer to achieving sustainability? Chem. Rev. 116 (2016) 7159–7329, https://doi.org/10.1021/acs.chemrev.6b00075.

[27] J. Lin, W. Tian, Z. Guan, H. Zhang, X. Duan, H. Wang, H. Sun, Y. Fang, Y. Huang, S. Wang, Functional carbon nitride materials in photo-fenton-like catalysis for

environmental remediation, Adv. Funct. Mater. 32 (2022), 2201743, https://doi.org/10.1002/adfm.202201743.

[28] H. Zhao, H. Yu, X. Quan, S. Chen, Y. Zhang, H. Zhao, H. Wang, Fabrication of atomic single layer graphitic-C3N4 and its high performance of photocatalytic disinfection under visible light irradiation, Appl. Catal. B (2014) 46–50, https://doi.org/10.1016/j.apcatb.2014.01.023, 152–153.

[29] S.N. Talapaneni, G. Singh, I.Y. Kim, K. AlBahily, A.H. Al-Muhtaseb, A.S. Karakoti, E. Tavakkoli, A. Vinu, Nanostructured carbon nitrides for CO$_2$ capture and conversion, Adv. Mater. 32 (2020), 1904635, https://doi.org/10.1002/adma.201904635.

[30] S.M. Ruban, K. Ramadass, G. Singh, S.N. Talapaneni, G. Kamalakar, C. R. Gadipelly, L.K. Mannepalli, Y. Sugi, A. Vinu, Organocatalysis with carbon nitrides, Sci. Technol. Adv. Mater. 24 (2023), 2188879, https://doi.org/10.1080/14686996.2023.2188879.

[31] V.W. Lau, B.V. Lotsch, A tour-guide through carbon nitride-land: structure- and dimensionality-dependent properties for photo(electro)chemical energy conversion and storage, Adv. Energy Mater. 12 (2022), 2101078, https://doi.org/10.1002/aenm.202101078.

[32] A. Savateev, S. Pronkin, J.D. Epping, M.G. Willinger, M. Antonietti, D. Dontsova, Synthesis of an electronically modified carbon nitride from a processable semiconductor, 3-amino-1,2,4-triazole oligomer, via a topotactic-like phase transition, J. Mater. Chem. 5 (2017) 8394–8401, https://doi.org/10.1039/C7TA01714F.

[33] H. May, Pyrolysis of melamine, J. Appl. Chem. 9 (1959) 340–344, https://doi.org/10.1002/jctb.5010090608.

[34] B. Jürgens, E. Irran, J. Senker, P. Kroll, H. Müller, W. Schnick, Melem (2,5,8-Triamino-tri-s-triazine), an important intermediate during condensation of melamine rings to graphitic carbon nitride: synthesis, structure determination by X-ray powder diffractometry, solid-state NMR, and theoretical studies, J. Am. Chem. Soc. 125 (2003) 10288–10300, https://doi.org/10.1021/ja0357689.

[35] L. Seyfarth, J. Senker, An NMR crystallographic approach for the determination of the hydrogen substructure of nitrogen bonded protons, Phys. Chem. Chem. Phys. 11 (2009) 3522–3531, https://doi.org/10.1039/B819319C.

[36] A. Sattler, S. Pagano, M. Zeuner, A. Zurawski, D. Gunzelmann, J. Senker, K. Müller-Buschbaum, W. Schnick, Melamine–Melem adduct phases: investigating the thermal condensation of melamine, Chemistry 15 (2009) 13161–13170, https://doi.org/10.1002/chem.200901518.

[37] B.V. Lotsch, M. Döblinger, J. Sehnert, L. Seyfarth, J. Senker, O. Oeckler, W. Schnick, Unmasking melon by a complementary approach employing electron diffraction, solid-state NMR spectroscopy, and theoretical calculations—structural characterization of a carbon nitride polymer, Chemistry 13 (2007) 4969–4980, https://doi.org/10.1002/chem.200601759.

[38] F.K. Kessler, Y. Zheng, D. Schwarz, C. Merschjann, W. Schnick, X. Wang, M. J. Bojdys, Functional carbon nitride materials — Design strategies for electrochemical devices, Nat. Rev. Mater. 2 (2017) 1–17, https://doi.org/10.1038/natrevmats.2017.30.

[39] M. Groenewolt, M. Antonietti, Synthesis of g-C3N4 nanoparticles in mesoporous silica host matrices, Adv. Mater. 17 (2005) 1789–1792, https://doi.org/10.1002/adma.200401756.

[40] T. Botari, W.P. Huhn, V.W. Lau, B.V. Lotsch, V. Blum, Thermodynamic equilibria in carbon nitride photocatalyst materials and conditions for the existence of graphitic carbon nitride g-C3N4, Chem. Mater. 29 (2017) 4445–4453, https://doi.org/10.1021/acs.chemmater.7b00965.

[41] F. Fina, S.K. Callear, G.M. Carins, J.T.S. Irvine, Structural investigation of graphitic carbon nitride via XRD and neutron diffraction, Chem. Mater. 27 (2015) 2612–2618, https://doi.org/10.1021/acs.chemmater.5b00411.

[42] X. Zhang, X. Xie, H. Wang, J. Zhang, B. Pan, Y. Xie, Enhanced photoresponsive ultrathin graphitic-phase C$_3$N$_4$ nanosheets for bioimaging, J. Am. Chem. Soc. 135 (2013) 18–21, https://doi.org/10.1021/ja308249k.

[43] Y. Wang, A. Vogel, M. Sachs, R.S. Sprick, L. Wilbraham, S.J.A. Moniz, R. Godin, M.A. Zwijnenburg, J.R. Durrant, A.I. Cooper, J. Tang, Current understanding and challenges of solar-driven hydrogen generation using polymeric photocatalysts, Nat. Energy 4 (2019) 746–760, https://doi.org/10.1038/s41560-019-0456-5.

[44] T.M. Clarke, J.R. Durrant, Charge photogeneration in organic solar cells, Chem. Rev. 110 (2010) 6736–6767, https://doi.org/10.1021/cr900271s.

[45] S. Melissen, T.Le Bahers, S.N. Steinmann, P. Sautet, Relationship between carbon nitride structure and exciton binding energies: a DFT perspective, J. Phys. Chem. 119 (2015) 25188–25196, https://doi.org/10.1021/acs.jpcc.5b07059.

[46] Y. Kang, Y. Yang, L.-C. Yin, X. Kang, G. Liu, H.-M. Cheng, An amorphous carbon nitride photocatalyst with greatly extended visible-light-responsive range for photocatalytic hydrogen generation, Adv. Mater. 27 (2015) 4572–4577, https://doi.org/10.1002/adma.201501939.

[47] F. Longobardo, G. Gentile, A. Criado, A. Actis, S. Colussi, V. Dal Santo, M. Chiesa, G. Filippini, P. Fornasiero, M. Prato, M. Melchionna, Tailored amorphization of graphitic carbon nitride triggers superior photocatalytic C–C coupling towards the synthesis of perfluoroalkyl derivatives, Mater. Chem. Front. 5 (2021) 7267–7275, https://doi.org/10.1039/D1QM01077H.

[48] A. Actis, M. Melchionna, G. Filippini, P. Fornasiero, M. Prato, E. Salvadori, M. Chiesa, Morphology and light-dependent spatial distribution of spin defects in carbon nitride, Angew. Chem. Int. Ed. 61 (2022), e202210640, https://doi.org/10.1002/anie.202210640.

[49] E. Raciti, S. Manoj Gali, M. Melchionna, G. Filippini, A. Actis, M. Chiesa, M. Bevilacqua, P. Fornasiero, M. Prato, D. Beljonne, R. Lazzaroni, Radical defects modulate the photocatalytic response in 2D-graphitic carbon nitride, Chem. Sci. 13 (2022) 9927–9939, https://doi.org/10.1039/D2SC03964H.

[50] A. Actis, M. Melchionna, G. Filippini, P. Fornasiero, M. Prato, M. Chiesa, E. Salvadori, Singlet-triplet energy inversion in carbon nitride photocatalysts, Angew. Chem. Int. Ed. (2023), e202313540, https://doi.org/10.1002/anie.202313540.

[51] O. Savateev, Photocharging of semiconductor materials: database, quantitative data analysis, and application in organic synthesis, Adv. Energy Mater. 12 (2022), 2200352, https://doi.org/10.1002/aenm.202200352.

[52] H. Schlomberg, J. Kröger, G. Savasci, M.W. Terban, S. Bette, I. Moudrakovski, V. Duppel, F. Podjaski, R. Siegel, J. Senker, R.E. Dinnebier, C. Ochsenfeld, B. V. Lotsch, Structural insights into poly(heptazine imides): a light-storing carbon nitride material for dark photocatalysis, Chem. Mater. 31 (2019) 7478–7486, https://doi.org/10.1021/acs.chemmater.9b02199.

[53] F. Podjaski, B.V. Lotsch, Optoelectronics meets optoionics: light storing carbon nitrides and beyond, Adv. Energy Mater. 11 (2021), 2003049, https://doi.org/10.1002/aenm.202003049.

[54] A. Savateev, D. Dontsova, B. Kurpil, M. Antonietti, Highly crystalline poly (heptazine imides) by mechanochemical synthesis for photooxidation of various organic substrates using an intriguing electron acceptor – Elemental sulfur, J. Catal. 350 (2017) 203–211, https://doi.org/10.1016/j.jcat.2017.02.029.

[55] D. Dontsova, S. Pronkin, M. Wehle, Z. Chen, C. Fettkenhauer, G. Clavel, M. Antonietti, Triazoles: a new class of precursors for the synthesis of negatively charged carbon nitride derivatives, Chem. Mater. 27 (2015) 5170–5179, https://doi.org/10.1021/acs.chemmater.5b00812.

[56] Z. Chen, A. Savateev, S. Pronkin, V. Papaefthimiou, C. Wolff, M.G. Willinger, E. Willinger, D. Neher, M. Antonietti, D. Dontsova, The easier the better" preparation of efficient photocatalysts—metastable poly(heptazine imide) salts, Adv. Mater. 29 (2017), 1700555, https://doi.org/10.1002/adma.201700555.

[57] K. Lu, Q. Wei, X. Bao, Z. Xiao, X. Cheng, X. Liu, Z. Wang, H. Li, B. Huang, Photocharged carbon nitride with local electron accumulation: towards outstanding round-the-clock hydrogen peroxide production, Appl. Surf. Sci. 609 (2023), 155242, https://doi.org/10.1016/j.apsusc.2022.155242.

[58] I. Krivtsov, D. Mitoraj, C. Adler, M. Ilkaeva, M. Sardo, L. Mafra, C. Neumann, A. Turchanin, C. Li, B. Dietzek, R. Leiter, J. Biskupek, U. Kaiser, C. Im, B. Kirchhoff, T. Jacob, R. Beranek, Water-soluble polymeric carbon nitride colloidal nanoparticles for highly selective quasi-homogeneous photocatalysis, Angew. Chem. Int. Ed. 59 (2020) 487–495, https://doi.org/10.1002/anie.201913331.

[59] C. Li, E. Hofmeister, I. Krivtsov, D. Mitoraj, C. Adler, R. Beranek, B. Dietzek, Photodriven charge accumulation and carrier dynamics in a water-soluble carbon nitride photocatalyst, ChemSusChem 14 (2021) 1728–1736, https://doi.org/10.1002/cssc.202002921.

[60] V.W. Lau, D. Klose, H. Kasap, F. Podjaski, M.-C. Pignié, E. Reisner, G. Jeschke, B. V. Lotsch, Dark photocatalysis: storage of solar energy in carbon nitride for time-delayed hydrogen generation, Angew. Chem. Int. Ed. 56 (2017) 510–514, https://doi.org/10.1002/anie.201608553.

[61] V.W. Lau, I. Moudrakovski, T. Botari, S. Weinberger, M.B. Mesch, V. Duppel, J. Senker, V. Blum, B.V. Lotsch, Rational design of carbon nitride photocatalysts by identification of cyanamide defects as catalytically relevant sites, Nat. Commun. 7 (2016) 12165, https://doi.org/10.1038/ncomms12165.

[62] Y. Zhang, A. Thomas, M. Antonietti, X. Wang, Activation of carbon nitride solids by protonation: morphology changes, enhanced ionic conductivity, and photoconduction experiments, J. Am. Chem. Soc. 131 (2009) 50–51, https://doi.org/10.1021/ja808329f.

[63] G. Chen, Z. Zhang, Y. Liao, Z. Zhang, Y. You, Modulating local charge distribution of carbon nitride for promoting exciton dissociation and charge-induced reactions, Small 17 (2021) 2100698, https://doi.org/10.1002/smll.202100698.

[64] Y. Markushyna, P. Lamagni, C. Teutloff, J. Catalano, N. Lock, G. Zhang, M. Antonietti, A. Savateev, Green radicals of potassium poly(heptazine imide) using light and benzylamine, J. Mater. Chem. 7 (2019) 24771–24775, https://doi.org/10.1039/C9TA09500D.

[65] H. Kasap, C.A. Caputo, B.C.M. Martindale, R. Godin, V.W. Lau, B.V. Lotsch, J. R. Durrant, E. Reisner, Solar-driven reduction of aqueous protons coupled to selective alcohol oxidation with a carbon nitride–molecular Ni catalyst system, J. Am. Chem. Soc. 138 (2016) 9183–9192, https://doi.org/10.1021/jacs.6b04325.

[66] J. Wang, P. Li, Y. Wang, Z. Liu, D. Wang, J. Liang, Q. Fan, New strategy for the persistent photocatalytic reduction of U(VI): utilization and storage of solar energy in K$^+$ and cyano co-decorated poly(heptazine imide), Adv. Sci. 10 (2023), 2205542, https://doi.org/10.1002/advs.202205542.

[67] F. Podjaski, J. Kröger, B.V. Lotsch, Toward an aqueous solar battery: direct electrochemical storage of solar energy in carbon nitrides, Adv. Mater. 30 (2018), 1705477, https://doi.org/10.1002/adma.201705477.

[68] A. Rogolino, O. Savateev, Photochargeable semiconductors: in "dark photocatalysis" and beyond, Adv. Funct. Mater. (2023), 2305028, https://doi.org/10.1002/adfm.202305028.

[69] C. Adler, S. Selim, I. Krivtsov, C. Li, D. Mitoraj, B. Dietzek, J.R. Durrant, R. Beranek, Photodoping and fast charge extraction in ionic carbon nitride photoanodes, Adv. Funct. Mater. 31 (2021), 2105369, https://doi.org/10.1002/adfm.202105369.

[70] H. Cheng, W. Sun, Y. Lu, H. Li, W. Su, J. Zhang, T. Guo, F. Li, P.S. Francis, Y. Zheng, Hot electrons in carbon nitride with ultra long lifetime and their application in reversible dynamic color displays, Cell Rep. Phys. Sci. 2 (2021), 100516, https://doi.org/10.1016/j.xcrp.2021.100516.

[71] P. Niu, L. Zhang, G. Liu, H.-M. Cheng, Graphene-like carbon nitride nanosheets for improved photocatalytic activities, Adv. Funct. Mater. 22 (2012) 4763–4770, https://doi.org/10.1002/adfm.201200922.

[72] V. Nicolosi, M. Chhowalla, M.G. Kanatzidis, M.S. Strano, J.N. Coleman, Liquid exfoliation of layered materials, Science 340 (2013), 1226419, https://doi.org/10.1126/science.1226419.

[73] T. Sano, S. Tsutsui, K. Koike, T. Hirakawa, Y. Teramoto, N. Negishi, K. Takeuchi, Activation of graphitic carbon nitride (g-C3N4) by alkaline hydrothermal treatment for photocatalytic NO oxidation in gas phase, J. Mater. Chem. 1 (2013) 6489–6496, https://doi.org/10.1039/C3TA10472A.

[74] Y. Chen, B. Wang, S. Lin, Y. Zhang, X. Wang, Activation of n → π* transitions in two-dimensional conjugated polymers for visible light photocatalysis, J. Phys. Chem. 118 (2014) 29981–29989, https://doi.org/10.1021/jp510187c.

[75] Y. Shiraishi, S. Kanazawa, Y. Sugano, D. Tsukamoto, H. Sakamoto, S. Ichikawa, T. Hirai, Highly selective production of hydrogen peroxide on graphitic carbon nitride (g-C3N4) photocatalyst activated by visible light, ACS Catal. 4 (2014) 774–780, https://doi.org/10.1021/cs401208c.

[76] H. Zhang, L.-H. Guo, L. Zhao, B. Wan, Y. Yang, Switching oxygen reduction pathway by exfoliating graphitic carbon nitride for enhanced photocatalytic phenol degradation, J. Phys. Chem. Lett. 6 (2015) 958–963, https://doi.org/10.1021/acs.jpclett.5b00149.

[77] J. Xu, L. Zhang, R. Shi, Y. Zhu, Chemical exfoliation of graphitic carbon nitride for efficient heterogeneous photocatalysis, J. Mater. Chem. 1 (2013) 14766–14772, https://doi.org/10.1039/C3TA13188B.

[78] S. Yang, Y. Gong, J. Zhang, L. Zhan, L. Ma, Z. Fang, R. Vajtai, X. Wang, P. M. Ajayan, Exfoliated graphitic carbon nitride nanosheets as efficient catalysts for hydrogen evolution under visible light, Adv. Mater. 25 (2013) 2452–2456, https://doi.org/10.1002/adma.201204453.

[79] E. Shahini, K. Shankar, T. Tang, Liquid-phase exfoliation of graphitic carbon nitrides studied by molecular dynamics simulation, J. Colloid Interface Sci. 630 (2023) 900–910, https://doi.org/10.1016/j.jcis.2022.10.150.

[80] Y. Xiao, G. Tian, W. Li, Y. Xie, B. Jiang, C. Tian, D. Zhao, H. Fu, Molecule self-assembly synthesis of porous few-layer carbon nitride for highly efficient photoredox catalysis, J. Am. Chem. Soc. 141 (2019) 2508–2515, https://doi.org/10.1021/jacs.8b12428.

[81] F. Goettmann, A. Fischer, M. Antonietti, A. Thomas, Chemical synthesis of mesoporous carbon nitrides using hard templates and their use as a metal-free catalyst for friedel–crafts reaction of benzene, Angew. Chem. Int. Ed. 45 (2006) 4467–4471, https://doi.org/10.1002/anie.200600412.

[82] X. Wang, K. Maeda, X. Chen, K. Takanabe, K. Domen, Y. Hou, X. Fu, M. Antonietti, Polymer semiconductors for artificial photosynthesis: hydrogen evolution by mesoporous graphitic carbon nitride with visible light, J. Am. Chem. Soc. 131 (2009) 1680–1681, https://doi.org/10.1021/ja809307s.

[83] X. Chen, Y.-S. Jun, K. Takanabe, K. Maeda, K. Domen, X. Fu, M. Antonietti, X. Wang, Ordered mesoporous SBA-15 type graphitic carbon nitride: a semiconductor host structure for photocatalytic hydrogen evolution with visible light, Chem. Mater. 21 (2009) 4093–4095, https://doi.org/10.1021/cm902130z.

[84] Y.-S. Jun, W.H. Hong, M. Antonietti, A. Thomas, Mesoporous, 2D hexagonal carbon nitride and titanium nitride/carbon composites, Adv. Mater. 21 (2009) 4270–4274, https://doi.org/10.1002/adma.200803500.

[85] S.S. Park, S.-W. Chu, C. Xue, D. Zhao, C.-S. Ha, Facile synthesis of mesoporous carbon nitrides using the incipient wetness method and the application as hydrogen adsorbent, J. Mater. Chem. 21 (2011) 10801, https://doi.org/10.1039/c1jm10849b.

[86] X.-H. Li, X. Wang, M. Antonietti, Mesoporous g-C3N4 nanorods as multifunctional supports of ultrafine metal nanoparticles: hydrogen generation from water and reduction of nitrophenol with tandem catalysis in one step, Chem. Sci. 3 (2012) 2170, https://doi.org/10.1039/c2sc20289a.

[87] X. Li, A.F. Masters, T. Maschmeyer, Photocatalytic hydrogen evolution from silica-templated polymeric graphitic carbon nitride-is the surface area important? ChemCatChem 7 (2015) 121–126, https://doi.org/10.1002/cctc.201402567.

[88] B. Long, Y. Zheng, L. Lin, K.A. Alamry, A.M. Asiri, X. Wang, Cubic mesoporous carbon nitride polymers with large cage-type pores for visible light photocatalysis, J. Mater. Chem. 5 (2017) 16179–16188, https://doi.org/10.1039/C6TA09802A.

[89] E.Z. Lee, Y.-S. Jun, W.H. Hong, A. Thomas, M.M. Jin, Cubic mesoporous graphitic Carbon(IV) nitride: an all-in-one chemosensor for selective optical sensing of metal ions, Angew. Chem. Int. Ed. 49 (2010) 9706–9710, https://doi.org/10.1002/anie.201004975.

[90] G.P. Mane, S.N. Talapaneni, K.S. Lakhi, H. Ilbeygi, U. Ravon, K. Al-Bahily, T. Mori, D. Park, A. Vinu, Highly ordered nitrogen-rich mesoporous carbon nitrides and their superior performance for sensing and photocatalytic hydrogen generation, Angew. Chem. Int. Ed. 56 (2017) 8481–8485, https://doi.org/10.1002/anie.201702386.

[91] I.Y. Kim, S. Kim, S. Premkumar, J. Yang, S. Umapathy, A. Vinu, Thermodynamically stable mesoporous C3N7 and C3N6 with ordered structure and their excellent performance for oxygen reduction reaction, Small 16 (2020), 1903572, https://doi.org/10.1002/smll.201903572.

[92] Y. Zheng, L. Lin, X. Ye, F. Guo, X. Wang, Helical graphitic carbon nitrides with photocatalytic and optical activities, Angew. Chem. Int. Ed. 53 (2014) 11926–11930, https://doi.org/10.1002/anie.201407319.

[93] X. Qian, X. Meng, J. Sun, L. Jiang, Y. Wang, J. Zhang, X. Hu, M. Shalom, J. Zhu, Salt-assisted synthesis of 3D porous g-C3N4 as a bifunctional photo- and electrocatalyst, ACS Appl. Mater. Interfaces 11 (2019) 27226–27232, https://doi.org/10.1021/acsami.9b08651.

[94] B. Yuan, Z. Chu, G. Li, Z. Jiang, T. Hu, Q. Wang, C. Wang, Water-soluble ribbon-like graphitic carbon nitride (g-C3N4): green synthesis, self-assembly and unique optical properties, J. Mater. Chem. 2 (2014) 8212–8215, https://doi.org/10.1039/C4TC01421A.

[95] K. Xiao, L. Chen, R. Chen, T. Heil, S.D.C. Lemus, F. Fan, L. Wen, L. Jiang, M. Antonietti, Artificial light-driven ion pump for photoelectric energy conversion, Nat. Commun. 10 (2019) 74, https://doi.org/10.1038/s41467-018-08029-5.

[96] K. Xiao, B. Tu, L. Chen, T. Heil, L. Wen, L. Jiang, M. Antonietti, Photo-driven ion transport for a photodetector based on an asymmetric carbon nitride nanotube membrane, Angew. Chem. Int. Ed. 58 (2019) 12574–12579, https://doi.org/10.1002/anie.201907833.

[97] S. Casanova, M.K. Borg, Y.M.J. Chew, D. Mattia, Surface-controlled water flow in nanotube membranes, ACS Appl. Mater. Interfaces 11 (2019) 1689–1698, https://doi.org/10.1021/acsami.8b18532.

[98] S.-W. Bian, Z. Ma, W.-G. Song, Preparation and characterization of carbon nitride nanotubes and their applications as catalyst supporter, J. Phys. Chem. 113 (2009) 8668–8672, https://doi.org/10.1021/jp810630k.

[99] X.-H. Li, J. Zhang, X. Chen, A. Fischer, A. Thomas, M. Antonietti, X. Wang, Condensed graphitic carbon nitride nanorods by nanoconfinement: promotion of crystallinity on photocatalytic conversion, Chem. Mater. 23 (2011) 4344–4348, https://doi.org/10.1021/cm201688v.

[100] C. Qiu, Y. Sun, Y. Xu, B. Zhang, X. Zhang, L. Yu, C. Su, Photoredox-catalyzed simultaneous olefin hydrogenation and alcohol oxidation over crystalline porous polymeric carbon nitride, ChemSusChem 14 (2021) 3344–3350, https://doi.org/10.1002/cssc.202101041.

[101] Y. Wang, X. Wang, M. Antonietti, Y. Zhang, Facile one-pot synthesis of nanoporous carbon nitride solids by using soft templates, ChemSusChem 3 (2010) 435–439, https://doi.org/10.1002/cssc.200900284.

[102] H. Yan, Soft-templating synthesis of mesoporous graphitic carbon nitride with enhanced photocatalytic H2 evolution under visible light, Chem. 48 (2012) 3430, https://doi.org/10.1039/c2cc00001f.

[103] Q. Fan, J. Liu, Y. Yu, S. Zuo, A template induced method to synthesize nanoporous graphitic carbon nitride with enhanced photocatalytic activity under visible light, RSC Adv. 4 (2014) 61877–61883, https://doi.org/10.1039/C4RA12033G.

[104] Z. Lin, X. Wang, Ionic liquid promoted synthesis of conjugated carbon nitride photocatalysts from urea, ChemSusChem 7 (2014) 1547–1550, https://doi.org/10.1002/cssc.201400016.

[105] Y. Zhang, T. Mori, J. Ye, M. Antonietti, Phosphorus-doped carbon nitride solid: enhanced electrical conductivity and photocurrent generation, J. Am. Chem. Soc. 132 (2010) 6294–6295, https://doi.org/10.1021/ja101749y.

[106] J. Xu, F. Wu, H.-T. Wu, B. Xue, Y.-X. Li, Y. Cao, Three-dimensional ordered mesoporous carbon nitride with large mesopores: synthesis and application towards base catalysis, Microporous Mesoporous Mater. 198 (2014) 223–229, https://doi.org/10.1016/j.micromeso.2014.07.042.

[107] Y. Cui, Z. Ding, X. Fu, X. Wang, Construction of conjugated carbon nitride nanoarchitectures in solution at low temperatures for photoredox catalysis, Angew. Chem. Int. Ed. 51 (2012) 11814–11818, https://doi.org/10.1002/anie.201206534.

[108] X. Xiao, Y. Gao, L. Zhang, J. Zhang, Q. Zhang, Q. Li, H. Bao, J. Zhou, S. Miao, N. Chen, J. Wang, B. Jiang, C. Tian, H. Fu, A promoted charge separation/transfer system from Cu single atoms and C3N4 layers for efficient photocatalysis, Adv. Mater. 32 (2020), 2003082, https://doi.org/10.1002/adma.202003082.

[109] J. Deng, F. Yao, L. Dai, X. Wue, H. Zhao, J. Bi, C. Fang, J. Zhu, J. Sun, Facilitating carrier separation of hierarchical carbon nitride by a nucleation processable strategy in photocatalytic H2 evolution, Appl. Surf. Sci. 615 (2023), 156325, https://doi.org/10.1016/j.apsusc.2023.156325.

[110] J. Barrio, A. Grafmüller, J. Tzadikov, M. Shalom, Halogen-hydrogen bonds: a general synthetic approach for highly photoactive carbon nitride with tunable properties, Appl. Catal. B 237 (2018) 681–688, https://doi.org/10.1016/j.apcatb.2018.06.043.

[111] X. Chu, X. Qu, A. Zada, L. Bai, Z. Li, F. Yang, L. Zhao, G. Zhang, X. Sun, Z. Yang, L. Jing, Ultrathin phosphate-modulated co phthalocyanine/g-C3N4 Heterojunction photocatalysts with single Co–N4 (II) sites for efficient O2 activation, Adv. Sci. 7 (2020), 2001543, https://doi.org/10.1002/advs.202001543.

[112] W. Yu, T. Zhang, Z. Zhao, Garland-like intercalated carbon nitride prepared by an oxalic acid-mediated assembly strategy for highly-efficient visible-light-driven photoredox catalysis, Appl. Catal. B 278 (2020), 119342, https://doi.org/10.1016/j.apcatb.2020.119342.

[113] J. Huang, W. Cheng, Y. Shi, G. Zeng, H. Yu, Y. Gu, L. Shi, K. Yi, Honeycomb-like carbon nitride through supramolecular preorganization of monomers for high photocatalytic performance under visible light irradiation, Chemosphere 211 (2018) 324–334, https://doi.org/10.1016/j.chemosphere.2018.07.171.

[114] Y. Liao, S. Zhu, J. Ma, Z. Sun, C. Yin, C. Zhu, X. Lou, D. Zhang, Tailoring the morphology of g-C3N4 by self-assembly towards high photocatalytic performance, ChemCatChem 6 (2014) 3419–3425, https://doi.org/10.1002/cctc.201402654.

[115] J. Sun, J. Xu, A. Grafmueller, X. Huang, C. Liedel, G. Algara-Siller, M. Willinger, C. Yang, Y. Fu, X. Wang, M. Shalom, Self-assembled carbon nitride for photocatalytic hydrogen evolution and degradation of p-nitrophenol, Appl. Catal. B 205 (2017) 1–10, https://doi.org/10.1016/j.apcatb.2016.12.030.

[116] H. Niu, W. Zhao, H. Lv, Y. Yang, Y. Cai, Accurate design of hollow/tubular porous g-C3N4 from melamine-cyanuric acid supramolecular prepared with mechanochemical method, Chem. Eng. J. 411 (2021), 128400, https://doi.org/10.1016/j.cej.2020.128400.

[117] T. Jordan, N. Fechler, J. Xu, T.J.K. Brenner, M. Antonietti, M. Shalom, Caffeine doping" of carbon/nitrogen-based organic catalysts: caffeine as a supramolecular edge modifier for the synthesis of photoactive carbon nitride tubes, ChemCatChem 7 (2015) 2826–2830, https://doi.org/10.1002/cctc.201500343.

[118] S. Dolai, N. Karjule, A. Azoulay, J. Barrio, Monomer sequence design at two solvent interface enables the synthesis of highly photoactive carbon nitride, RSC Adv. 9 (2019) 26091–26096, https://doi.org/10.1039/C9RA05264J.

[119] Q. Liang, Z. Li, Z.-H. Huang, F. Kang, Q.-H. Yang, Holey graphitic carbon nitride nanosheets with carbon vacancies for highly improved photocatalytic hydrogen production, Adv. Funct. Mater. 25 (2015) 6885–6892, https://doi.org/10.1002/adfm.201503221.

[120] G.A. Tompsett, W.C. Conner, K.S. Yngvesson, Microwave synthesis of nanoporous materials, Chemistry 7 (2006) 296–319, https://doi.org/10.1002/cphc.200500449.

[121] A. Torres-Pinto, C.G. Silva, J.L. Faria, A.M.T. Silva, The effect of precursor selection on the microwave-assisted synthesis of graphitic carbon nitride, Catal. Today 424 (2023), 113868, https://doi.org/10.1016/j.cattod.2022.08.010.

[122] M. Marchi, E. Raciti, S.M. Gali, F. Piccirilli, H. Vondracek, A. Actis, E. Salvadori, C. Rosso, A. Criado, C. D'Agostino, D. Lee, A.C. Foucher, R.K. Rai, D. Beljonne, E.A. Stach, M. Chiesa, R. Lazzaroni, G. Filippini, M. Prato, M. Melchionna, P. Fornasiero, Carbon vacancies steer the activity in dual Ni carbon nitride photocatalysis, Adv. Sci. (2023), 2303781, https://doi.org/10.1002/advs.202303781.

[123] C. Huang, Y. Wen, J. Ma, D. Dong, Y. Shen, S. Liu, H. Ma, Y. Zhang, Unraveling fundamental active units in carbon nitride for photocatalytic oxidation reactions, Nat. Commun. 12 (2021) 320, https://doi.org/10.1038/s41467-020-20521-5.

[124] H. Yu, R. Shi, Y. Zhao, T. Bian, Y. Zhao, C. Zhou, L.Z. Wu, C.-H. Tung, T. Zhang, Alkali-assisted synthesis of nitrogen deficient graphitic carbon nitride with tunable band structures for efficient visible-light-driven hydrogen evolution, Adv. Mater. 29 (2017), 1605148, https://doi.org/10.1002/adma.201605148.

[125] L. Shi, L. Yang, W. Zhou, Y. Liu, L. Yin, X. Hai, H. Song, J. Ye, Photoassisted construction of holey defective g-C $_3$N $_4$ photocatalysts for efficient visible-light-driven H $_2$ O $_2$ production, Small 14 (2018), 1703142, https://doi.org/10.1002/smll.201703142.

[126] P. Niu, L.-C. Yin, Y.-Q. Yang, G. Liu, H.-M. Cheng, Increasing the visible light absorption of graphitic carbon nitride (melon) photocatalysts by homogeneous self-modification with nitrogen vacancies, Adv. Mater. 26 (2014) 8046–8052, https://doi.org/10.1002/adma.201404057.

[127] G. Filippini, F. Longobardo, L. Forster, A. Criado, G. Di Carmine, L. Nasi, C. D'Agostino, M. Melchionna, P. Fornasiero, M. Prato, Light-driven, heterogeneous organocatalysts for C–C bond formation toward valuable perfluoroalkylated intermediates, Sci. Adv. 6 (2020) eabc9923, https://doi.org/10.1126/sciadv.abc9923.

[128] M. Shalom, M. Guttentag, C. Fettkenhauer, S. Inal, D. Neher, A. Llobet, M. Antonietti, *In Situ* formation of heterojunctions in modified graphitic carbon nitride: synthesis and noble metal free photocatalysis, Chem. Mater. 26 (2014) 5812–5818, https://doi.org/10.1021/cm503258z.

[129] J. Barrio, L. Lin, X. Wang, M. Shalom, Design of a unique energy-band structure and morphology in a carbon nitride photocatalyst for improved charge separation and hydrogen production, ACS Sustain. Chem. Eng. 6 (2018) 519–530, https://doi.org/10.1021/acssuschemeng.7b02807.

[130] Y. Yang, Y. Chen, Z. Li, S. Tang, Y. Li, Z. Fu, S. Yang, M. Yang, H. Xie, Homojunction type of carbon nitride as a robust photo-catalyst for reduction conversion of CO2 in water vapor under visible light, Chem. Eng. J. 430 (2022), 132668, https://doi.org/10.1016/j.cej.2021.132668.

[131] J. Li, B. Shen, Z. Hong, B. Lin, B. Gao, Y. Chen, A facile approach to synthesize novel oxygen-doped g-C3N4 with superior visible-light photoreactivity, Chem. 48 (2012) 12017, https://doi.org/10.1039/c2cc35862j.

[132] J. Oh, R.J. Yoo, S.Y. Kim, Y.J. Lee, D.W. Kim, S. Park, Oxidized carbon nitrides: water-dispersible, atomically thin carbon nitride-based nanodots and their performances as bioimaging probes, Chem. Eur. J. 21 (2015) 6241–6246, https://doi.org/10.1002/chem.201406151.

[133] P. Choudhary, A. Bahuguna, A. Kumar, S.S. Dhankhar, C.M. Nagaraja, V. Krishnan, Oxidized graphitic carbon nitride as a sustainable metal-free catalyst for hydrogen transfer reactions under mild conditions, Green Chem. 22 (2020) 5084–5095, https://doi.org/10.1039/D0GC01123A.

[134] X. Song, X. Li, X. Zhang, Y. Wu, C. Ma, P. Huo, Y. Yan, Fabricating C and O co-doped carbon nitride with intramolecular donor-acceptor systems for efficient photoreduction of CO2 to CO, Appl. Catal. B 268 (2020), 118736, https://doi.org/10.1016/j.apcatb.2020.118736.

[135] Y. Chen, Y. Qu, P. Xu, X. Zhou, J. Sun, Insight into the influence of donor-acceptor system on graphitic carbon nitride nanosheets for transport of photoinduced charge carriers and photocatalytic H2 generation, J. Colloid Interface Sci. 601 (2021) 326–337, https://doi.org/10.1016/j.jcis.2021.05.145.

[136] L. Jiang, X. Yuan, Y. Pan, J. Liang, G. Zeng, Z. Wu, H. Wang, Doping of graphitic carbon nitride for photocatalysis: a review, Appl. Catal. B 217 (2017) 388–406, https://doi.org/10.1016/j.apcatb.2017.06.003.

[137] S. Guo, Z. Deng, M. Li, B. Jiang, C. Tian, Q. Pan, H. Fu, Phosphorus-doped carbon nitride tubes with a layered micro-nanostructure for enhanced visible-light photocatalytic hydrogen evolution, Angew. Chem. Int. Ed. 55 (2016) 1830–1834, https://doi.org/10.1002/anie.201508505.

[138] J. Ran, T.Y. Ma, G. Gao, X.-W. Du, S.Z. Qiao, Porous P-doped graphitic carbon nitride nanosheets for synergistically enhanced visible-light photocatalytic H $_2$ production, Energy Environ. Sci. 8 (2015) 3708–3717, https://doi.org/10.1039/C5EE02650D.

[139] J. Ma, D. Jin, X. Yang, S. Sun, J. Zhou, R. Sun, Phosphorus-doped carbon nitride with grafted sulfonic acid groups for efficient photocatalytic synthesis of xylonic acid, Green Chem. 23 (2021) 4150–4160, https://doi.org/10.1039/D1GC00920F.

[140] G. Liu, P. Niu, C. Sun, S.C. Smith, Z. Chen, G.Q. (Max) Lu, H.-M. Cheng, Unique electronic structure induced high photoreactivity of sulfur-doped graphitic C $_3$N $_4$, J. Am. Chem. Soc. 132 (2010) 11642–11648, https://doi.org/10.1021/ja103798k.

[141] G. Li, Y. Wu, M. Wang, W. Zhou, X. Liu, Z. Zhu, X. Song, P. Huo, Graphitic carbon nitride modified with 2-Aminothiophene-3-Carbonitrile to boost molecular dipole and $n \rightarrow \pi^*$ electronic transition for photoreduction of carbon dioxide, ACS Appl. Nano Mater. 6 (2023) 14513–14526, https://doi.org/10.1021/acsanm.3c02600.

[142] Z. Lin, X. Wang, Nanostructure engineering and doping of conjugated carbon nitride semiconductors for hydrogen photosynthesis, Angew. Chem. Int. Ed. 52 (2013) 1735–1738, https://doi.org/10.1002/anie.201209017.

[143] C. Feng, L. Tang, Y. Deng, J. Wang, J. Luo, Y. Liu, X. Ouyang, H. Yang, J. Yu, J. Wang, Synthesis of leaf-vein-like g-C $_3$N $_4$ with tunable band structures and charge transfer properties for selective photocatalytic H $_2$ O $_2$ evolution, Adv. Funct. Mater. 30 (2020), 2001922, https://doi.org/10.1002/adfm.202001922.

[144] G. Zhang, M. Zhang, X. Ye, X. Qiu, S. Lin, X. Wang, Iodine modified carbon nitride semiconductors as visible light photocatalysts for hydrogen evolution, Adv. Mater. 26 (2014) 805–809, https://doi.org/10.1002/adma.201303611.

[145] Z.-A. Lan, G. Zhang, X. Wang, A facile synthesis of Br-modified g-C3N4 semiconductors for photoredox water splitting, Appl. Catal. B 192 (2016) 116–125, https://doi.org/10.1016/j.apcatb.2016.03.062.

[146] D. Wang, X. Huang, Y. Huang, X. Yu, Y. Lei, X. Dong, Z. Su, Self-assembly synthesis of petal-like Cl-doped g-C3N4 nanosheets with tunable band structure for enhanced photocatalytic activity, Colloids Surf. A 611 (2021), 125780, https://doi.org/10.1016/j.colsurfa.2020.125780.

[147] W. Zou, X.-H. Liu, C. Xue, X.-T. Zhou, H.-Y. Yu, P. Fan, H.-B. Ji, Enhancement of the visible-light absorption and charge mobility in a zinc porphyrin polymer/g-C3N4 heterojunction for promoting the oxidative coupling of amines, Appl. Catal. B 285 (2021), 119863, https://doi.org/10.1016/j.apcatb.2020.119863.

[148] S.K. Kaiser, Z. Chen, D. Faust Akl, S. Mitchell, J. Pérez-Ramírez, Single-atom catalysts across the periodic table, Chem. Rev. 120 (2020) 11703–11809, https://doi.org/10.1021/acs.chemrev.0c00576.

[149] Y. Xia, M. Sayed, L. Zhang, B. Cheng, J. Yu, Single-atom heterogeneous photocatalysts, Chem. Catalysis 1 (2021) 1173–1214, https://doi.org/10.1016/j.checat.2021.08.009.

[150] V.B. Saptal, V. Ruta, M.A. Bajada, G. Vilé, Single-atom catalysis in organic synthesis, Angew. Chem. Int. Ed. (2022), e202219306, https://doi.org/10.1002/anie.202219306 n/a (n.d.).

[151] G. Gentile, M. Marchi, M. Melchionna, P. Fornasiero, M. Prato, G. Filippini, Use of carbon nitrides as photoactive supports in single-atom heterogeneous catalysis for synthetic purposes, J. Org. Chem. 2022 (2022), https://doi.org/10.1002/ejoc.202200944.

[152] G.F.S.R. Rocha, M.A.R. Da Silva, A. Rogolino, G.A.A. Diab, L.F.G. Noleto, M. Antonietti, I.F. Teixeira, Carbon nitride based materials: more than just a support for single-atom catalysis, Chem. Soc. Rev. 52 (2023) 4878–4932, https://doi.org/10.1039/D2CS00806H.

[153] X. Wang, X. Chen, A. Thomas, X. Fu, M. Antonietti, Metal-containing carbon nitride compounds: a new functional organic-metal hybrid material, Adv. Mater. 21 (2009) 1609–1612, https://doi.org/10.1002/adma.200802627.

[154] Y. Cao, S. Chen, Q. Luo, H. Yan, Y. Lin, W. Liu, L. Cao, J. Lu, J. Yang, T. Yao, S. Wei, Atomic-level insight into optimizing the hydrogen evolution pathway over a Co $_1$ -N $_4$ single-site photocatalyst, Angew. Chem. Int. Ed. 56 (2017) 12191–12196, https://doi.org/10.1002/anie.201706467.

[155] Z. Zhu, X. Tang, T. Wang, W. Fan, Z. Liu, C. Li, P. Huo, Y. Yan, Insight into the effect of co-doped to the photocatalytic performance and electronic structure of g-C3N4 by first principle, Appl. Catal. B 241 (2019) 319–328, https://doi.org/10.1016/j.apcatb.2018.09.009.

[156] Z. Ding, X. Chen, M. Antonietti, X. Wang, Synthesis of transition metal-modified carbon nitride polymers for selective hydrocarbon oxidation, ChemSusChem (2010) 274–281, https://doi.org/10.1002/cssc.201000149.

[157] M.A.R. da Silva, I.F. Silva, Q. Xue, B.T.W. Lo, N.V. Tarakina, B.N. Nunes, P. Adler, S.K. Sahoo, D.W. Bahnemann, N. López-Salas, A. Savateev, C. Ribeiro, T. D. Kühne, M. Antonietti, I.F. Teixeira, Sustainable oxidation catalysis supported by light: fe-poly (heptazine imide) as a heterogeneous single-atom photocatalyst, Appl. Catal. B 304 (2022), 120965, https://doi.org/10.1016/j.apcatb.2021.120965.

[158] S.K. Sahoo, I.F. Teixeira, A. Naik, J. Heske, D. Cruz, M. Antonietti, A. Savateev, T. D. Kühne, Photocatalytic water splitting reaction catalyzed by ion-exchanged salts of potassium poly(heptazine imide) 2D materials, J. Phys. Chem. 125 (2021) 13749–13758, https://doi.org/10.1021/acs.jpcc.1c03947.

[159] L. Xing, Q. Yang, C. Zhu, Y. Bai, Y. Tang, M. Rueping, Y. Cai, Poly(heptazine imide) ligand exchange enables remarkable low catalyst loadings in heterogeneous metallaphotocatalysis, Nat. Commun. 14 (2023) 1501, https://doi.org/10.1038/s41467-023-37113-8.

[160] D. Sun, Y. Chen, X. Yu, Y. Yin, G. Tian, Engineering high-coordinated cerium single-atom sites on carbon nitride nanosheets for efficient photocatalytic amine oxidation and water splitting into hydrogen, Chem. Eng. J. 462 (2023), 142084, https://doi.org/10.1016/j.cej.2023.142084.

[161] S.K. Verma, R. Verma, Y.R. Girish, F. Xue, L. Yan, S. Verma, M. Singh, Y. Vaishnav, A.B. Shaik, R.R. Bhandare, K.P. Rakesh, K.S.S. Kumar, K. S. Rangappa, Heterogeneous graphitic carbon nitrides in visible-light-initiated organic transformations, Green Chem. 24 (2022) 438–479, https://doi.org/10.1039/D1GC03490A.

[162] A. Savateev, M. Antonietti, Heterogeneous organocatalysis for photoredox chemistry, ACS Catal. 8 (2018) 9790–9808, https://doi.org/10.1021/acscatal.8b02595.

[163] A. Savateev, I. Ghosh, B. König, M. Antonietti, Photoredox catalytic organic transformations using heterogeneous carbon nitrides, Angew. Chem. Int. Ed. 57 (2018) 15936–15947, https://doi.org/10.1002/anie.201802472.

[164] G. Marcì, E.I. García-López, L. Palmisano, Polymeric carbon nitride (C3N4) as heterogeneous photocatalyst for selective oxidation of alcohols to aldehydes, Catal. Today 315 (2018) 126–137, https://doi.org/10.1016/j.cattod.2018.03.038.

[165] M.J. Cocero, 9.4 - Supercritical Water Oxidation (SCWO). Application to Industrial Wastewater Treatment, Elsevier, 2001, pp. 509–526, https://doi.org/10.1016/S0926-9614(01)80030-7. A. Bertucco, G. Vetter (Eds.), Industrial Chemistry Library.

[166] Y. Wang, H. Li, J. Yao, X. Wang, M. Antonietti, Synthesis of boron doped polymeric carbon nitride solids and their use as metal-free catalysts for aliphatic C–H bond oxidation, Chem. Sci. 2 (2011) 446–450, https://doi.org/10.1039/C0SC00475H.

[167] Bond Dissociation Energies, Atomic Charges, Bond Properties, and Molecular Energies, John Wiley & Sons, Ltd, 2008, pp. 151–166, https://doi.org/10.1002/9780470405918.ch12.

[168] L. Kesavan, R. Tiruvalam, M.H. Ab Rahim, M.I. bin Saiman, D.I. Enache, R. L. Jenkins, N. Dimitratos, J.A. Lopez-Sanchez, S.H. Taylor, D.W. Knight, C. J. Kiely, G.J. Hutchings, Solvent-free oxidation of primary carbon-hydrogen bonds in toluene using Au-Pd alloy nanoparticles, Science 331 (2011) 195–199, https://doi.org/10.1126/science.1198468.

[169] F. Konietzni, U. Kolb, U. Dingerdissen, W.F. Maier, AMM-MnxSi-catalyzed selective oxidation of toluene, J. Catal. 176 (1998) 527–535, https://doi.org/10.1006/jcat.1998.2076.

[170] X.-H. Li, X. Wang, M. Antonietti, Solvent-free and metal-free oxidation of toluene using O2 and g-C3N4 with nanopores: nanostructure boosts the catalytic selectivity, ACS Catal. 2 (2012) 2082–2086, https://doi.org/10.1021/cs300413x.

[171] F. Ding, P. Chen, F. Liu, L. Chen, J.-K. Guo, S. Shen, Q. Zhang, L.-H. Meng, C.-T. Au, S.-F. Yin, Bi2MoO6/g-C3N4 of 0D/2D heterostructure as efficient photocatalyst for selective oxidation of aromatic alkanes, Appl. Surf. Sci. 490 (2019) 102–108, https://doi.org/10.1016/j.apsusc.2019.06.057.

[172] P. Chen, Y. Li, C. Xiao, L. Chen, J.-K. Guo, S. Shen, C.-T. Au, S.-F. Yin, Preparation of Helical BiVO4/Ag/C3N4 for selective oxidation of C–H Bond under visible light irradiation, ACS Sustain. Chem. Eng. 7 (2019) 17500–17506, https://doi.org/10.1021/acssuschemeng.9b04858.

[173] H.-H. Zhang, Z.-C. Zhou, Y.-J. Dong, L. Zhang, H.-Y. Chen, D.-B. Kuang, Constructing a Cs3Sb2Br9/g-C3N4 hybrid for photocatalytic aromatic C(sp3)□H bond activation, Sol. RRL 5 (2021), 2100559, https://doi.org/10.1002/solr.202100559.

[174] S.K. Pahari, R.-A. Doong, Few-layered phosphorene–graphitic carbon nitride nanoheterostructure as a metal-free photocatalyst for aerobic oxidation of benzyl alcohol and toluene, ACS Sustain. Chem. Eng. 8 (2020) 13342–13351, https://doi.org/10.1021/acssuschemeng.0c04078.

[175] W. Zhang, A. Bariotaki, I. Smonou, F. Hollmann, Visible-light-driven photooxidation of alcohols using surface-doped graphitic carbon nitride, Green Chem. 19 (2017) 2096–2100, https://doi.org/10.1039/C7GC00539C.

[176] G.A. Russell, Deuterium-isotope effects in the autoxidation of aralkyl hydrocarbons. Mechanism of the interaction of peroxy radicals1, J. Am. Chem. Soc. 79 (1957) 3871–3877, https://doi.org/10.1021/ja01571a068.

[177] P. Geng, T. Tang, G. Pan, W. Wang, J. Hu, Y. Cai, A g-C3N4-based heterogeneous catalyst for visible light mediated aerobic benzylic C–H oxygenations, Green Chem. 21 (2019) 6116–6122, https://doi.org/10.1039/C9GC02870F.

[178] M. Hosseini-Sarvari, Z. Akrami, Visible-light assisted of nano Ni/g-C3N4 with efficient photocatalytic activity and stability for selective aerobic C–H activation and epoxidation, J. Organomet. Chem. 928 (2020) 121549, https://doi.org/10.1016/j.jorganchem.2020.121549.

[179] R. Cao, M.-Q. Zhang, C. Hu, D. Xiao, M. Wang, D. Ma, Catalytic oxidation of polystyrene to aromatic oxygenates over a graphitic carbon nitride catalyst, Nat. Commun. 13 (2022) 4809, https://doi.org/10.1038/s41467-022-32510-x.

[180] R. Ghalta, R. Bal, R. Srivastava, Metal-free photocatalytic transformation of waste polystyrene into valuable chemicals: advancing sustainability through circular economy, Green Chem. 25 (2023) 7318–7334, https://doi.org/10.1039/D3GC02591H.

[181] P. Zhang, Y. Wang, J. Yao, C. Wang, C. Yan, M. Antonietti, H. Li, Visible-light-induced metal-free allylic oxidation utilizing a coupled photocatalytic system of g-C3N4 and N-Hydroxy compounds, Adv. Synth. Catal. 353 (2011) 1447–1451, https://doi.org/10.1002/adsc.201100175.

[182] F. Recupero, C. Punta, Free radical functionalization of organic compounds catalyzed by N-Hydroxyphthalimide, Chem. Rev. 107 (2007) 3800–3842, https://doi.org/10.1021/cr040170k.

[183] K. Weissermel, H.-J. Arpe, Industrial Organic Chemistry, John Wiley & Sons, 2008.

[184] H. Grennberg, J.-E. Bäckvall, Allylic Oxidations, in: Transition Metals for Organic Synthesis, John Wiley & Sons, Ltd, 2004, pp. 243–265, https://doi.org/10.1002/9783527619405.ch5c.

[185] C. Bartocci, A. Maldotti, G. Varani, P. Battioni, V. Carassiti, D. Mansuy, Photoredox and photocatalytic characteristics of various iron meso-tetraarylporphyrins, Inorg. Chem. 30 (1991) 1255–1259, https://doi.org/10.1021/ic00006a018.

[186] Z. Yang, Q. Zhang, L. Ren, X. Chen, D. Wang, L. Liu, J. Ye, Efficient photocatalytic conversion of CH4 into ethanol with O2 over nitrogen vacancy-rich carbon nitride at room temperature, Chem. 57 (2021) 871–874, https://doi.org/10.1039/D0CC07397K.

[187] Y. Zhang, L. Hu, C. Zhu, J. Liu, H. Huang, Y. Liu, Z. Kang, Air activation by a metal-free photocatalyst for "totally-green" hydrocarbon selective oxidation, Catal. Sci. Technol. 6 (2016) 7252–7258, https://doi.org/10.1039/C6CY01066K.

[188] X.-H. Li, J.-S. Chen, X. Wang, J. Sun, M. Antonietti, Metal-free activation of dioxygen by graphene/g-C3N4 nanocomposites: functional dyads for selective oxidation of saturated hydrocarbons, J. Am. Chem. Soc. 133 (2011) 8074–8077, https://doi.org/10.1021/ja200997a.

[189] G. Sportelli, G. Grando, M. Bevilacqua, G. Filippini, M. Melchionna, P. Fornasiero, Graphitic carbon nitride as photocatalyst for the direct formylation of anilines, Chemistry (2023), https://doi.org/10.1002/chem.202301718 n/a (n.d.) e202301718.

[190] A. Galushchinskiy, Y. Zou, J. Odutola, P. Nikačević, J.-W. Shi, N. Tkachenko, N. López, P. Farràs, O. Savateev, Insights into the role of graphitic carbon nitride as a photobase in proton-coupled electron transfer in (sp3)C–H oxygenation of oxazolidinones, Angew. Chem. Int. Ed. 62 (2023), e202301815, https://doi.org/10.1002/anie.202301815.

[191] L. Möhlmann, S. Blechert, Carbon nitride-catalyzed photoredox sakurai reactions and allylborations, Adv. Synth. Catal. 356 (2014) 2825–2829, https://doi.org/10.1002/adsc.201400551.

[192] G. Sportelli, G. Grando, M. Bevilacqua, G. Filippini, M. Melchionna, P. Fornasiero, Graphitic carbon nitride as photocatalyst for the direct formylation of anilines, Chem. Eur. J. (2023), e202301718, https://doi.org/10.1002/chem.202301718 n/a.

[193] S. Yang, P. Li, Z. Wang, L. Wang, Photoinduced oxidative formylation of N, N -dimethylanilines with molecular oxygen without external photocatalyst, Org. Lett. 19 (2017) 3386–3389, https://doi.org/10.1021/acs.orglett.7b01230.

[194] T. Ghosh, A. Das, B. König, Photocatalytic N-formylation of amines via a reductive quenching cycle in the presence of air, Org. Biomol. Chem. 15 (2017) 2536–2540, https://doi.org/10.1039/C7OB00250E.

[195] L. Akyuz, An imine based COF as a smart carrier for targeted drug delivery: from synthesis to computational studies, Microporous Mesoporous Mater. 294 (2020), 109850, https://doi.org/10.1016/j.micromeso.2019.109850.

[196] S.-I. Murahashi, Synthetic aspects of metal-catalyzed oxidations of amines and related reactions, Angew. Chem. Int. Ed. Engl. 34 (1995) 2443–2465, https://doi.org/10.1002/anie.199524431.

[197] S.F. Martin, Recent applications of imines as key intermediates in the synthesis of alkaloids and novel nitrogen heterocycles, Pure Appl. Chem. 81 (2009) 195–204, https://doi.org/10.1351/PAC-CON-08-07-03.

[198] S. Kobayashi, Y. Mori, J.S. Fossey, M.M. Salter, Catalytic enantioselective formation of C–C bonds by addition to imines and hydrazones: a ten-year update, Chem. Rev. 111 (2011) 2626–2704, https://doi.org/10.1021/cr100204f.

[199] J. Yang, M. Xu, J. Wang, S. Jin, B. Tan, A facile approach to prepare multiple heteroatom-doped carbon materials from imine-linked porous organic polymers, Sci. Rep. 8 (2018) 4200, https://doi.org/10.1038/s41598-018-22507-2.

[200] F. Su, S.C. Mathew, L. Möhlmann, M. Antonietti, X. Wang, S. Blechert, Aerobic oxidative coupling of amines by carbon nitride photocatalysis with visible light, Angew. Chem. 123 (2011) 683–686, https://doi.org/10.1002/ange.201004365.

[201] M.A. Bajada, A. Vijeta, A. Savateev, G. Zhang, D. Howe, E. Reisner, Visible-light flow reactor packed with porous carbon nitride for aerobic substrate oxidations, ACS Appl. Mater. Interfaces 12 (2020) 8176–8182, https://doi.org/10.1021/acsami.9b19718.

[202] D. Zhang, X. Han, T. Dong, X. Guo, C. Song, Z. Zhao, Promoting effect of cyano groups attached on g-C3N4 nanosheets towards molecular oxygen activation for visible light-driven aerobic coupling of amines to imines, J. Catal. 366 (2018) 237–244, https://doi.org/10.1016/j.jcat.2018.08.018.

[203] Y. Wang, J. Zhou, X. Hao, Y. Wang, Z. Zou, Fabricating direct Z-scheme PTCDA/g-C3N4 photocatalyst based on interfacial strong interaction for efficient photooxidation of benzylamine, Appl. Surf. Sci. 456 (2018) 861–870, https://doi.org/10.1016/j.apsusc.2018.06.181.

[204] S. Zhang, K. Chen, W. Peng, J. Huang, g-C3N4/Uio-66-NH2 nanocomposites with enhanced visible light photocatalytic activity for hydrogen evolution and oxidation of amines to imines, New J. Chem. 44 (2020) 3052–3061, https://doi.org/10.1039/C9NJ05495B.

[205] A. Kumar, P. Kumar, C. Joshi, S. Ponnada, A.K. Pathak, A. Ali, B. Sreedhar, S. L. Jain, A [Fe(bpy)3]2+ grafted graphitic carbon nitride hybrid for visible light assisted oxidative coupling of benzylamines under mild reaction conditions, Green Chem. 18 (2016) 2514–2521, https://doi.org/10.1039/C5GC02090E.

[206] Y. Xu, Y. Chen, W.-F. Fu, Visible-light driven oxidative coupling of amines to imines with high selectivity in air over core-shell structured CdS@C3N4, Appl. Catal. B 236 (2018) 176–183, https://doi.org/10.1016/j.apcatb.2018.03.098.

[207] A. Yuan, H. Lei, Z. Wang, X. Dong, Improved photocatalytic performance for selective oxidation of amines to imines on graphitic carbon nitride/bismuth tungstate heterojunctions, J. Colloid Interface Sci. 560 (2020) 40–49, https://doi.org/10.1016/j.jcis.2019.10.060.

[208] S. Mondal, L. Sahoo, Y. Vaishnav, S. Mishra, R.S. Roy, C.P. Vinod, A.K. De, U. K. Gautam, Wavelength dependent luminescence decay kinetics in 'quantum-confined' g-C3N4 nanosheets exhibiting high photocatalytic efficiency upon plasmonic coupling, J. Mater. Chem. 8 (2020) 20581–20592, https://doi.org/10.1039/D0TA08001B.

[209] F. Su, S.C. Mathew, G. Lipner, X. Fu, M. Antonietti, S. Blechert, X. Wang, mpg-C3N4-catalyzed selective oxidation of alcohols using O2 and visible light, J. Am. Chem. Soc. 132 (2010) 16299–16301, https://doi.org/10.1021/ja102866p.

[210] O. Savateev, Selective Oxidation of Alcohols Using Carbon Nitride Photocatalysts, in: UV–Visible Photocatalysis for Clean Energy Production and Pollution Remediation, John Wiley & Sons, Ltd, 2023, pp. 27–40, https://doi.org/10.1002/9783527837991.ch3.

[211] R. Sheldon, Metal-Catalyzed Oxidations of Organic Compounds: Mechanistic Principles and Synthetic Methodology Including Biochemical Processes, Elsevier, 2012.

[212] D.I. Enache, J.K. Edwards, P. Landon, B. Solsona-Espriu, A.F. Carley, A. A. Herzing, M. Watanabe, C.J. Kiely, D.W. Knight, G.J. Hutchings, Solvent-free oxidation of primary alcohols to aldehydes using Au-Pd/TiO2 catalysts, Science 311 (2006) 362–365, https://doi.org/10.1126/science.1120560.

[213] U.R. Pillai, E. Sahle-Demessie, Oxidation of alcohols over Fe3+/montmorillonite-K10 using hydrogen peroxide, Appl. Catal. A 245 (2003) 103–109, https://doi.org/10.1016/S0926-860X(02)00617-8.

[214] I. Krivtsov, M. Ilkaeva, E.I. García-López, G. Marcì, L. Palmisano, E. Bartashevich, E. Grigoreva, K. Matveeva, E. Díaz, S. Ordóñez, Effect of substituents on partial photocatalytic oxidation of aromatic alcohols assisted by polymeric C3N4, ChemCatChem 11 (2019) 2713–2724, https://doi.org/10.1002/cctc.201900362.

[215] A. Amini, M. Karimi, M. Rabbani, V. Safarifard, Cobalt-doped g-C3N4/MOF heterojunction composite with tunable band structures for photocatalysis aerobic oxidation of benzyl alcohol, Polyhedron 216 (2022), 115728, https://doi.org/10.1016/j.poly.2022.115728.

[216] Z. Yang, X. Xu, X. Liang, C. Lei, Y. Cui, W. Wu, Y. Yang, Z. Zhang, Z. Lei, Construction of heterostructured MIL-125/Ag/g-C3N4 nanocomposite as an efficient bifunctional visible light photocatalyst for the organic oxidation and reduction reactions, Appl. Catal. B 205 (2017) 42–54, https://doi.org/10.1016/j.apcatb.2016.12.012.

[217] C. Xiao, L. Zhang, H. Hao, W. Wang, High selective oxidation of benzyl alcohol to benzylaldehyde and benzoic acid with surface oxygen vacancies on W18O49/holey ultrathin g-C3N4 nanosheets, ACS Sustain. Chem. Eng. 7 (2019) 7268–7276, https://doi.org/10.1021/acssuschemeng.9b00299.

[218] X. Chu, Y. Qu, A. Zada, L. Bai, Z. Li, F. Yang, L. Zhao, G. Zhang, X. Sun, Z.-D. Yang, L. Jing, Ultrathin phosphate-modulated Co phthalocyanine/g-C3N4 heterojunction photocatalysts with single Co–N4 (II) sites for efficient O2 activation, Adv. Sci. 7 (2020), 2001543, https://doi.org/10.1002/advs.202001543.

[219] L. Sun, B. Li, X. Chu, N. Sun, Y. Qu, X. Zhang, I. Khan, L. Bai, L. Jing, Synthesis of Si–O-bridged g-C3N4/WO3 2D-heterojunctional nanocomposites as efficient photocatalysts for aerobic alcohol oxidation and mechanism insight, ACS Sustain. Chem. Eng. 7 (2019) 9916–9927, https://doi.org/10.1021/acssuschemeng.9b00711.

[220] S.M. Hosseini, M. Karimi, V. Safarifard, Metal–organic framework/carbon nitride nanosheets composites (TMU-49/CNNSs): efficient photocatalyst for aerobic oxidation of alcohols under visible light, New J. Chem. 45 (2021) 17674–17682, https://doi.org/10.1039/D1NJ02369A.

[221] H. Liang, J. Wang, B. Jin, D. Li, Y. Men, Direct growth of Au nanoparticles on g-C3N4 for photocatalytic selective alcohol oxidations, Chem. 109 (2019), 107574, https://doi.org/10.1016/j.inoche.2019.107574.

[222] C. Yang, B. Wang, L. Zhang, L. Yin, X. Wang, Synthesis of layered carbonitrides from biotic molecules for photoredox transformations, Angew. Chem. Int. Ed. 56 (2017) 6627–6631, https://doi.org/10.1002/anie.201702213.

[223] Y. Chen, J. Zhang, M. Zhang, X. Wang, Molecular and textural engineering of conjugated carbon nitride catalysts for selective oxidation of alcohols with visible light, Chem. Sci. 4 (2013) 3244–3248, https://doi.org/10.1039/C3SC51203G.

[224] B. Long, Z. Ding, X. Wang, Carbon nitride for the selective oxidation of aromatic alcohols in water under visible light, ChemSusChem 6 (2013) 2074–2078, https://doi.org/10.1002/cssc.201300360.

[225] J. Ding, W. Xu, H. Wan, D. Yuan, C. Chen, L. Wang, G. Guan, W.-L. Dai, Nitrogen vacancy engineered graphitic C3N4-based polymers for photocatalytic oxidation of aromatic alcohols to aldehydes, Appl. Catal. B 221 (2018) 626–634, https://doi.org/10.1016/j.apcatb.2017.09.048.

[226] L. Zhang, D. Liu, J. Guan, X. Chen, X. Guo, F. Zhao, T. Hou, X. Mu, Metal-free g-C3N4 photocatalyst by sulfuric acid activation for selective aerobic oxidation of benzyl alcohol under visible light, Mater. Res. Bull. 59 (2014) 84–92, https://doi.org/10.1016/j.materresbull.2014.06.021.

[227] M. Bellardita, E.I. García-López, G. Marcì, I. Krivtsov, J.R. García, L. Palmisano, Selective photocatalytic oxidation of aromatic alcohols in water by using P-doped g-C3N4, Appl. Catal. B 220 (2018) 222–233, https://doi.org/10.1016/j.apcatb.2017.08.033.

[228] B. Zhang, T.-J. Zhao, H.-H. Wang, Enhanced photocatalytic activity of aerogel composed of crooked carbon nitride nanolayers with nitrogen vacancies, ACS Appl. Mater. Interfaces 11 (2019) 34922–34929, https://doi.org/10.1021/acsami.9b10123.

[229] S. Mazzanti, G. Manfredi, A.J. Barker, M. Antonietti, A. Savateev, P. Giusto, Carbon nitride thin films as all-in-one technology for photocatalysis, ACS Catal. 11 (2021) 11109–11116, https://doi.org/10.1021/acscatal.1c02909.

[230] Y. Markushyna, C.M. Schüßlbauer, T. Ullrich, D.M. Guldi, M. Antonietti, A. Savateev, Chromoselective synthesis of sulfonyl chlorides and sulfonamides with potassium poly(heptazine imide) photocatalyst, Angew. Chem. Int. Ed. 60 (2021) 20543–20550, https://doi.org/10.1002/anie.202106183.

[231] L. Luo, X. Xiao, Q. Li, S. Wang, Y. Li, J. Hou, B. Jiang, Engineering of single atomic Cu-N3 active sites for efficient singlet oxygen production in photocatalysis, ACS Appl. Mater. Interfaces 13 (2021) 58596–58604, https://doi.org/10.1021/acsami.1c17782.

[232] H. Wang, S. Jiang, S. Chen, D. Li, X. Zhang, W. Shao, X. Sun, J. Xie, Z. Zhao, Q. Zhang, Y. Tian, Y. Xie, Enhanced singlet oxygen generation in oxidized graphitic carbon nitride for organic synthesis, Adv. Mater. 28 (2016) 6940–6945, https://doi.org/10.1002/adma.201601413.

[233] S. Samanta, S. Khilari, D. Pradhan, R. Srivastava, An Efficient, Visible light driven, selective oxidation of aromatic alcohols and amines with O2 using BiVO4/g-C3N4 nanocomposite: a systematic and comprehensive study toward the development of a photocatalytic process, ACS Sustain. Chem. Eng. 5 (2017) 2562–2577, https://doi.org/10.1021/acssuschemeng.6b02902.

[234] C. Wang, Q. Wan, J. Cheng, S. Lin, A. Savateev, M. Antonietti, X. Wang, Efficient aerobic oxidation of alcohols to esters by acidified carbon nitride photocatalysts, J. Catal. 393 (2021) 116–125, https://doi.org/10.1016/j.jcat.2020.11.021.

[235] S. Verma, R.B. Nasir Baig, M.N. Nadagouda, R.S. Varma, Photocatalytic CH activation and oxidative esterification using Pd@g-C3N4, Catal. Today 309 (2018) 248–252, https://doi.org/10.1016/j.cattod.2017.06.009.

[236] M.A. Khan, I.F. Teixeira, M.M.J. Li, Y. Koito, S.C.E. Tsang, Graphitic carbon nitride catalysed photoacetalization of aldehydes/ketones under ambient conditions, Chem. 52 (2016) 2772–2775, https://doi.org/10.1039/C5CC08344C.

[237] H. Zhan, W. Liu, M. Fu, J. Cen, J. Lin, H. Cao, Carbon nitride-catalyzed oxidative cleavage of carbon–carbon bond of α-hydroxy ketones with visible light and thermal radiation, Appl. Catal. A 468 (2013) 184–189, https://doi.org/10.1016/j.apcata.2013.08.008.

[238] A. Rajagopalan, M. Lara, W. Kroutil, Oxidative alkene cleavage by chemical and enzymatic methods, Adv. Synth. Catal. 355 (2013) 3321–3335, https://doi.org/10.1002/adsc.201300882.

[239] V. Balzani, A. Credi, M. Venturi, Photochemical conversion of solar energy, ChemSusChem 1 (2008) 26–58, https://doi.org/10.1002/cssc.200700087.

[240] Y. Zhang, N. Hatami, N.S. Lange, E. Ronge, W. Schilling, C. Jooss, S. Das, A metal-free heterogeneous photocatalyst for the selective oxidative cleavage of CC bonds in aryl olefins via harvesting direct solar energy, Green Chem. 22 (2020) 4516–4522, https://doi.org/10.1039/D0GC01187H.

[241] H. Wang, R. Jia, M. Hong, H. Miao, B. Ni, T. Niu, Hydroxyl radical-mediated oxidative cleavage of CC bonds and further esterification reaction by heterogeneous semiconductor photocatalysis, Green Chem. 23 (2021) 6591–6597, https://doi.org/10.1039/D1GC01931G.

[242] I. Camussi, B. Mannucci, A. Speltini, A. Profumo, C. Milanese, L. Malavasi, P. Quadrelli, g-C3N4 - Singlet oxygen made easy for organic synthesis: scope and limitations, ACS Sustain. Chem. Eng. 7 (2019) 8176–8182, https://doi.org/10.1021/acssuschemeng.8b06164.

[243] A. Studer, D.P. Curran, Catalysis of radical reactions: a radical chemistry perspective, Angew. Chem. Int. Ed. 55 (2016) 58–102, https://doi.org/10.1002/anie.201505090.

[244] W. Jiang, H. Deng, J. Liu, Efficient photocatalytic aerobic oxidations by a molecular cobalt catalyst linked to mesoporous carbon nitride, Catal. Commun. 170 (2022), 106498, https://doi.org/10.1016/j.catcom.2022.106498.

[245] J. Legros, J.R. Dehli, C. Bolm, Applications of catalytic asymmetric sulfide oxidations to the syntheses of biologically active sulfoxides, Adv. Synth. Catal. 347 (2005) 19–31, https://doi.org/10.1002/adsc.200404206.

[246] E.G. Mata, Recent advances in the synthesis of sulfoxides from sulfides, phosphorus, sulfur, and silicon and the related elements. 117 (1996) 231–286. https://doi.org/10.1080/10426509608038790.

[247] Z. Xie, W. Wang, X. Ke, X. Cai, X. Chen, S. Wang, W. Lin, X. Wang, A heptazine-based polymer photocatalyst with donor-acceptor configuration to promote exciton dissociation and charge separation, Appl. Catal. B 325 (2023), 122312, https://doi.org/10.1016/j.apcatb.2022.122312.

[248] Y. Xu, Z.-C. Fu, S. Cao, Y. Chen, W.-F. Fu, Highly selective oxidation of sulfides on a CdS/C3N4 catalyst with dioxygen under visible-light irradiation, Catal. Sci. Technol. 7 (2017) 587–595, https://doi.org/10.1039/C6CY01568A.

[249] X. Chen, K. Deng, P. Zhou, Z. Zhang, Metal- and additive-free oxidation of sulfides into sulfoxides by fullerene-modified carbon nitride with visible-light illumination, ChemSusChem 11 (2018) 2444–2452, https://doi.org/10.1002/cssc.201800450.

[250] P. Zhang, Y. Wang, H. Li, M. Antonietti, Metal-free oxidation of sulfides by carbon nitride with visible light illumination at room temperature, Green Chem. 14 (2012) 1904–1908, https://doi.org/10.1039/C2GC35148J.

[251] E.L. Clennan, Persulfoxide: key intermediate in reactions of singlet oxygen with sulfides, Acc. Chem. Res. 34 (2001) 875–884, https://doi.org/10.1021/ar0100879.

[252] J. Li, Z. An, J. Sun, C. Tan, D. Gao, Y. Tan, Y. Jiang, Highly selective oxidation of organic sulfides by a conjugated polymer as the photosensitizer for singlet oxygen generation, ACS Appl. Mater. Interfaces 12 (2020) 35475–35481, https://doi.org/10.1021/acsami.0c10162.